Growth-Driven Deformation of Ultra-Soft Tissues

A thesis submitted in fulfilment of the requirements

for the degree of Master of Technology

by

Divya Adil

18807252

DEPARTMENT OF MECHANICAL ENGINEERING

INDIAN INSTITUTE OF TECHNOLOGY KANPUR

May 2023

18807252

Certificate

It is certified that the work contained in this thesis entitled "Growth-Driven Deformation of Ultra-Soft Tissues" by "Divya Adil" has been carried out under my supervision and that it has not been submitted elsewhere for a degree.

Prof. Sumit Basu

Professor

Department of Mechanical Engineering

Indian Institute of Technology Kanpur

May 2023

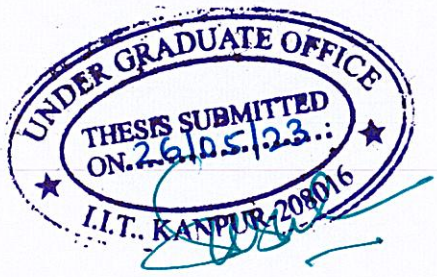

Declaration

This is to certify that the thesis titled "Growth-Driven Deformation of Ultra-Soft Tissues" has been authored by me. It presents the research conducted by me under the supervision of Prof. Sumit Basu.

To the best of my knowledge, it is an original work, both in terms of research content and narrative, and has not been submitted elsewhere, in part or in full, for a degree. Further, due credit has been attributed to the relevant state-of-the-art and collaborations (if any) with appropriate citations and acknowledgements, in line with established norms and practices.

Divya Adil

Programme: M. Tech

Department of Mechanical Engineering

Indian Institute of Technology Kanpur

208016

May 2023

Abstract

Name of the student: **Divya Adil** Roll No: **18807252**

Degree for which submitted: **M.Tech.** Department: **Mechanical Engineering**

Thesis title: **Growth-Driven Deformation of Ultra-Soft Tissues**

Thesis supervisor: **Prof. Sumit Basu**

Month and year of thesis submission: **May 2023**

Physical constraints on growing tissues are frequently observed in biological systems and contribute to changes in form. This phenomenon plays a crucial role in the development of various structures (morphogenesis) in organisms. One such constraint is differential growth, which leads to deformation and buckling in several scenarios, such as rippled leaf edges, folding of intestinal walls, and the buckling of the forebrain roof plate, resulting in the formation of two cerebral hemispheres. In this thesis, we apply the principles of continuum mechanics to elucidate how growth influences deformation in 3D structures.

We model the tissue as a growing hyperelastic mass and utilize the software ABAQUS for numerical analyses. To introduce three-dimensional growth in the tissues and calculate the stresses developed, we have developed a user subroutine program (UMAT). Initially, we employ simple geometries and compare the deformations and stresses with analytical solutions to validate our numerical model. Subsequently, we perform simulations on more complex cases involving folding and investigate the types of growth that lead to tissue buckling.

Acknowledgements

I sincerely thank my thesis supervisor, Prof. Sumit Basu, for making this work possible. I have learned a lot from him about the field and research skills in general, such as problem-solving and maintaining patience when progress is slow. I will carry these lessons with me in my future pursuits.

I am deeply grateful to Prof. Amitabha Bandyopadhyay, who initially informed me about this collaborative project. Without his assistance, my academic path would have likely taken a different direction.

I am delighted to have had the opportunity to learn from and work with Prof. Jonaki Sen. It has been a wonderful experience and has provided me with greater clarity regarding my future aspirations.

Despite the devastating ramifications of the pandemic, it served as the driving force for me to explore fields beyond my department, and I am extremely pleased with how things have turned out.

I would not have been able to complete either of my degrees without the unwavering support of my family and friends. My family has consistently supported and encouraged me in my academic pursuits, for which I am eternally grateful. My friends have stood by me through the highs and lows, even after most of them graduated and moved away, and I am incredibly thankful to have them in my life. Additionally, I feel fortunate to have such friendly and welcoming labmates who have made my time in the lab thoroughly enjoyable.

I am also immensely grateful for the sports facilities on campus and the student-run clubs and societies in which I have participated. They have played a crucial role in managing stress and keeping me content.

Contents

List of Figures

Dedicated to Youtube Music and my trusty headphones for making even the monotonous tasks a 'jamming' experience

Chapter 1

Introduction

1.1 Background to the Problem

The growth of soft biological tissues and the process by which they form different structures (morphogenesis) can be studied at different length scales and through different perspectives. The more dominant view of growth and morphogenesis is at the cellular and molecular level, which looks at how biomolecular interactions drive the process. However, it can also be viewed at the organ level from a continuum mechanics perspective, which is what we are trying to employ. This continuum perspective couples the processes of growth, or change in mass, and morphogenesis, change in form which is often not seen in other approaches.[2]

Physical constraints on growing tissues are often seen in biological systems and lead to changes in form (like bending, folding or wrinkling). Consider two rods of the same length attached to each other along the length. If the bottom rod grows faster in length than the top rod, both will bend such that the bottom rod has a larger radius of curvature. Similarly, in two dimensions, if we have a circular sheet which first grows uniformly but then grows with a higher radial growth rate than circumferential, it will grow into a hat shape. In comparison, if the circumferential growth is higher than the radial, it will tend to form wrinkles on the circumference.[13] These are illustrated in Figure 1.2.

This kind of differential or constrained growth can be seen in several common systems. The leaves of several plants have a rippled edge rather than a flat one due to differential growth.[7] Our small intestine's innermost layer has finger-like projections called villi, which are formed due to restricted, differential growth.[12] Our brain buckles to form the

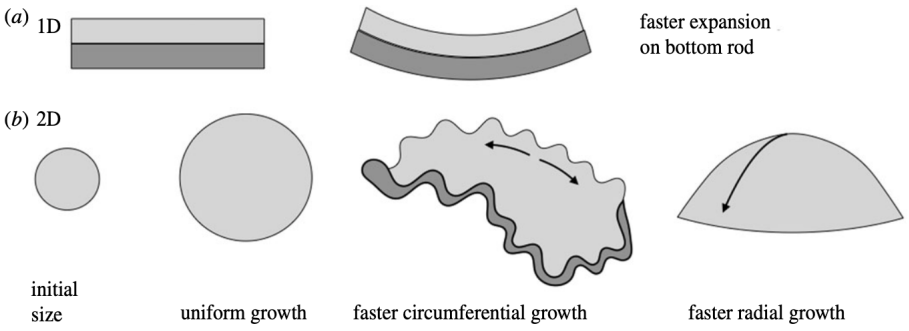

FIGURE 1.1: Buckling in (a) one-dimension (rods) and (b) two-dimensions (circular sheet) due to differential growth [13]

two hemispheres due to higher growth of the inner layer compared to the outer layer. In this work, we have created a mathematical model that describes the growth-driven deformation of soft tissues in 3 dimensions. We have implemented it numerically on different geometries to replicate some naturally occurring phenomena.

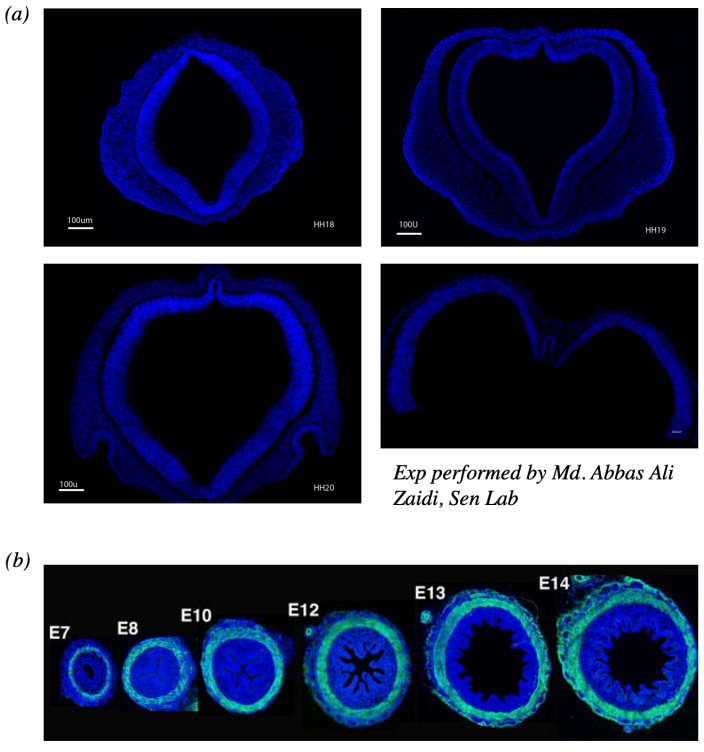

FIGURE 1.2: Examples of growth driven buckling in soft tissues. (a) cross section of chick forebrain at stages HH18, HH19, HH20 and HH21 (b) cross section of chick gut from stages E7 to E14 showing formation of villi.[12]

We have built on previous work by the lab on a particular 2-dimensional folding problem.[6] The 2-dimensional model was specific to the forebrain buckling problem and considered only a tangential growth rate. We have extended it to work for a general growth rate in any direction that leads to deformation, and a model that is not specific to a particular problem but can be applied to several scenarios.

1.2 Overview of the Thesis

Soft tissues are modelled as a continuum elastic body that deforms as a hyperelastic material. Since the tissue is soft and the deformations large, finite deformation theory is applied. Rodrigues et al.[11] introduced the concept of multiplicative decomposition of the total deformation into growth and elastic deformation, which we have utilised in our model. Chapter 2 of this thesis presents the laws and equations governing the system. These include the cell number and mass balance and linear and angular momentum balance. Applying these laws and several assumptions for biological tissues gives us constraints on the growth part of the deformation gradient. We then used hyperelastic theory to calculate the expressions for stresses, and linearised it to get the tangent stiffness matrix for implementation on ABAQUS. Chapter 3 presents some analytically solvable test cases with isotropic growth that we have used to validate the model by comparing the numerical and analytical solutions. Chapter 4 moves on to simple buckling cases with anisotropic growth that cannot be solved easily analytically, where we use our model to reproduce some published results. We conclude with a summary of the work and future directions.

Chapter 2

Continuum Description and Finite Element Formulation of the Problem

We are modelling the soft tissue as a continuum, as it is being looked at at a length scale where it is a valid assumption. Since these tissues are very soft and undergo large deformations, we assume that it follows hyperelastic theory. Since most tissues have a lot of water stored in them, it makes them practically incompressible, which is an assumption we apply in the later stages of developing our model. We use balance laws and multiplicative decomposition of the deformation gradient, along with these and some other assumptions to build our model.

2.1 Multiplicative Decomposition of the Deformation Gradient

The deformation gradient tensor is defined to take a point from the reference configuration to the current configuration as shown below:

$$d\mathbf{x} = \mathbf{F} \cdot d\mathbf{X} \tag{2.1}$$

The deformation of the tissue is due to two factors - growth of mass and elastic deformation. Hence, the deformation can be visualised to occur via an intermediate configuration. The

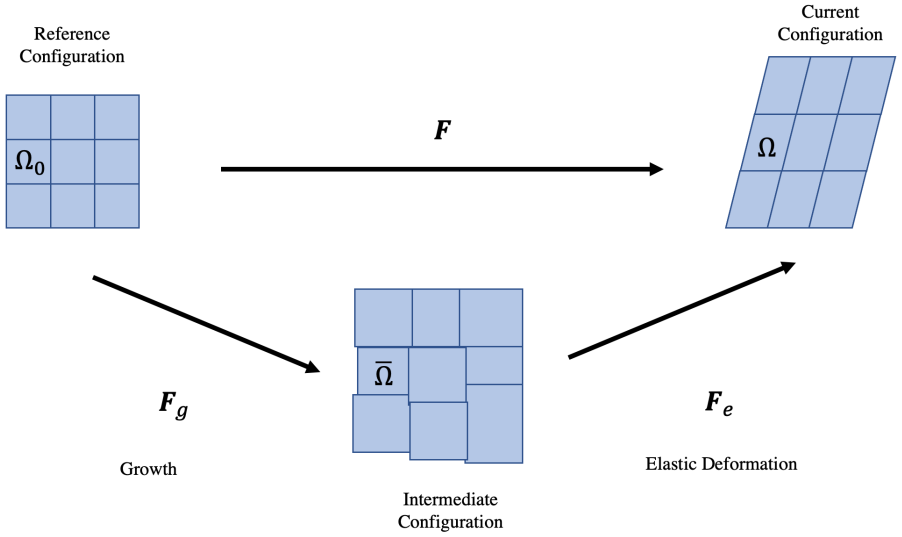

FIGURE 2.1: Reference, Intermediate and Current configurations

tissue deforms due to growth from the reference to the intermediate configuration, and due to elastic deformation from the intermediate to the current configuration. The deformation gradient can therefore be decomposed into two components - $\mathbf{F}^g$ or the growth part of the deformation gradient and $\mathbf{F}^e$ or the elastic part of the deformation gradient. This is the multiplicative decomposition proposed by Rodriguez et al.[11] The two decomposed components are related as follows, where $d\mathbf{x}^g$ is the point in the intermediate configuration.

$$d\mathbf{x}^g = \mathbf{F}^g \cdot d\mathbf{X} \tag{2.2}$$

$$d\mathbf{x} = \mathbf{F}^e \cdot d\mathbf{x}^g \tag{2.3}$$

From the above equations, we obtain the following relation.

$$\mathbf{F} = \mathbf{F}^e \cdot \mathbf{F}^g \tag{2.4}$$

2.2 Balance Laws

The reference configuration Ω_0 undergoes growth to give the intermediate configuration $\bar{\Omega}$ which deforms hyperelastically due to the geometric constraints on growth to give the

current configuration Ω as shown in Figure 2.1.

2.2.1 Balance of Mass and the Continuity Equation

Let the density in the reference, intermediate and current configuration be given as ρ_0, $\bar{\rho}$ and ρ respectively. The mass dm_0 of an infinitesimal volume dV_0 in the reference configuration is

$$dm_0 = \rho_0 dV_0.$$

Since there is no growth between the intermediate and the current configurations,

$$dm = d\bar{m} \Rightarrow \bar{\rho} d\bar{V} = \rho dV.$$

If r_0, $\bar{r}$ and r are the time rates of mass addition in the reference, intermediate and current configurations respectively, the mass balance equation can be given as the following.

$$\begin{aligned} \int_\Omega dm &= \int_{\Omega_0} dm_0 + \int_{\Omega_0} \left(\int_0^t r_0 d\tau \right) dV_0 \\ \Rightarrow \int_\Omega \rho dV &= \int_{\Omega_0} \rho_0 dV_0 + \int_{\Omega_0} \left(\int_0^t r_0 d\tau \right) dV_0 \end{aligned}$$

Changing the domain to reference volume,

$$\int_{\Omega_0} \rho J dV_0 = \int_{\Omega_0} \rho_0 dV_0 + \int_{\Omega_0} \left(\int_0^t r_0 d\tau \right) dV_0.$$

Using the localisation argument, we get

$$\rho J = \rho_0 + \int_0^t r_0 d\tau.$$

Let $\rho J = \rho_g^0$, which signifies current mass per unit reference volume. This gives us $\dfrac{D(\rho J)}{Dt} = \dfrac{D(\rho_g^0)}{Dt} = r_0$. Since the total rate of mass addition over the whole volume in any configuration remains the same,

$$\int_{\Omega} r dV = \int_{\Omega_0} r_0 dV_0$$
$$\Rightarrow \int_{\Omega_0} r J dV_0 = \int_{\Omega_0} r_0 dV_0$$

Using the localisation argument, this gives us

$$r_0 = rJ \tag{2.5}$$

The mass balance condition finally gives us a relation between the mass growth rates in different configurations. The differential form of the mass balance gives us the continuity equation as follows:

$$\begin{aligned}
&\frac{D}{Dt}\int_{\Omega} dm = \int_{\Omega} r dV \\
\Rightarrow &\frac{D}{Dt}\int_{\Omega} \rho dV = \int_{\Omega} r dV \\
\Rightarrow &\frac{D}{Dt}\int_{\Omega_0} \rho J dV_0 = \int_{\Omega_0} r J dV_0 \\
\Rightarrow &\int_{\Omega_0} \left(\frac{D\rho}{Dt} J + \rho \frac{DJ}{Dt}\right) dV_0 = \int_{\Omega_0} r J dV_0
\end{aligned}$$

Since $\frac{DJ}{Dt} = J\text{tr}\mathbf{L} = J\text{tr}\mathbf{D}$, we get

$$\int_{\Omega_0} \left(\frac{D\rho}{Dt} + \rho \text{tr}\mathbf{D}\right) J dV_0 = \int_{\Omega_0} r J dV_0$$

When we change the domain of integration back to the reference configuration

$$\int_{\Omega} \left(\frac{D\rho}{Dt} + \rho \text{tr}\mathbf{D}\right) dV = \int_{\Omega} r dV$$

Applying the localisation argument, we finally get

$$\frac{D\rho}{Dt} + \rho \text{tr}\mathbf{D} = r$$

Or,

$$\frac{D\rho}{Dt} + \rho \mathrm{tr}(\dot{\mathbf{F}}\mathbf{F}^{-1}) = r \tag{2.6}$$

Similarly, when we consider the continuity equation between the intermediate and current configurations, we get

$$\frac{D\bar{\rho}}{Dt} + \bar{\rho} \mathrm{tr}(\dot{\mathbf{F}}_\mathbf{g}\mathbf{F}_\mathbf{g}^{-1}) = rJ_e \tag{2.7}$$

Since, $\mathbf{F} = \mathbf{F_e}\mathbf{F_g}$, we can find tr$\mathbf{L}$ as

$$\mathbf{L} = \dot{\mathbf{F}}\mathbf{F}^{-1} = \left(\dot{\mathbf{F}}_\mathbf{e}\mathbf{F_g} + \mathbf{F_e}\dot{\mathbf{F}}_\mathbf{g}\right)\mathbf{F_g}^{-1}\mathbf{F_e}^{-1} = \dot{\mathbf{F}}_\mathbf{e}\mathbf{F_e}^{-1} + \mathbf{F_e}\dot{\mathbf{F}}_\mathbf{g}\mathbf{F_g}^{-1}\mathbf{F_e}^{-1}$$

The trace of the velocity gradient tensor therefore becomes

$$\mathrm{tr}\mathbf{L} = \mathrm{tr}(\dot{\mathbf{F}}_\mathbf{e}\mathbf{F_e}^{-1}) + \mathrm{tr}(\mathbf{F_e}\dot{\mathbf{F}}_\mathbf{g}\mathbf{F_g}^{-1}\mathbf{F_e}^{-1}) \tag{2.8}$$

Using this result along with the continuity equations and the fact that $\bar{\rho} = \rho J_e$, we get the following two equations:

$$\frac{D\bar{\rho}}{Dt} + \bar{\rho} \mathrm{tr}(\dot{\mathbf{F}}_\mathbf{g}\mathbf{F_g}^{-1}) = J_e\left(\frac{D\rho}{Dt} + \rho \mathrm{tr}(\dot{\mathbf{F}}\mathbf{F}^{-1})\right) \tag{2.9}$$

$$\frac{D\bar{\rho}}{Dt} = J_e\frac{D\rho}{Dt} + \bar{\rho} \mathrm{tr}(\dot{\mathbf{F}}_\mathbf{e}\mathbf{F_e}^{-1}) \tag{2.10}$$

These equations will further be simplified using additional assumptions to give us conditions on the form of the growth such that it satisfies mass balance.

2.2.2 Cell number Balance and Density Preserving Growth

Now, applying balancing the cell number gives us the relation between mass growth rates and cell division and cell death (apoptosis) rates. If n is the number of cells per unit volume, or cell number density, $\mathbf{v}$ is the cell flow velocity, and k_d and k_a are the numbers

of cell divisions and deaths per unit volume respectively, we get the following equation for cell number balance

$$\frac{Dn}{Dt} + n\nabla \cdot \mathbf{v} = (k_d - k_a)n$$

Assuming that the average cell mass is M_c and the average cell mass density and volume are ρ_c and Ω_c respectively, we get the following relation from the cell number balance equation.

$$n(t) = \frac{\rho(t)}{M_c(t)}$$

$$\begin{aligned}
&\frac{D}{Dt}(\frac{\rho}{M_c}) + \frac{\rho}{M_c}\nabla \cdot \mathbf{v} = (k_d - k_a)\,\frac{\rho}{M_c} \\
\Rightarrow &M_c\left(\frac{\frac{D\rho}{Dt}M_c - \rho\frac{DM_c}{Dt}}{M_c^2}\right) + \rho\nabla \cdot \mathbf{v} = (k_d - k_a)\,\rho \\
\Rightarrow &\frac{D\rho}{Dt} - \frac{\rho}{M_c}\frac{DM_c}{Dt} + \rho\nabla \cdot \mathbf{v} = (k_d - k_a)\,\rho \\
\Rightarrow &\frac{D\rho}{Dt} + \rho\nabla \cdot \mathbf{v} = (k_d - k_a)\,\rho + \frac{\rho}{M_c}\frac{DM_c}{Dt}
\end{aligned}$$

Now, if we use the fact that $\mathrm{tr}\mathbf{L} = \mathrm{tr}(\frac{\partial \mathbf{v}}{\partial \mathbf{x}}) = \nabla \cdot \mathbf{v}$, it gives us

$$\frac{D\rho}{Dt} + \rho\mathrm{tr}\mathbf{D} = (k_d - k_a)\,\rho + \frac{\rho}{M_c}\frac{DM_c}{Dt}$$

On comparing this with the continuity equation, we get the following relation between the mass addition rate and the cell division and apoptosis rates

$$r = (k_d - k_a)\,\rho + \frac{\rho}{M_c}\frac{DM_c}{Dt}$$

If we assume that the average mass of the cell does not change with time and that the mass growth is only due to a net increase in cell number, we get

$$r = (k_d - k_a)\,\rho$$

We assume that the cells do not grow in size but only multiply in number. This means that the number of cells in a unit volume, or the density remains constant, and it is the volume that increases. If we assume that the growth is density preserving, that is $\bar{\rho} = \rho_0 \Rightarrow \frac{D\bar{\rho}}{Dt} = 0$, the continuity equations become

$$\begin{aligned} J_e \frac{D\rho}{Dt} + \bar{\rho}\mathrm{tr}(\dot{\mathbf{F}}_\mathbf{e}\mathbf{F}_\mathbf{e}^{-\mathbf{1}}) &= 0 \\ \Rightarrow J_e \frac{D\rho}{Dt} + \rho J_e \mathrm{tr}(\dot{\mathbf{F}}_\mathbf{e}\mathbf{F}_\mathbf{e}^{-\mathbf{1}}) &= 0 \\ \Rightarrow \frac{D\rho}{Dt} + \rho \mathrm{tr}(\dot{\mathbf{F}}_\mathbf{e}\mathbf{F}_\mathbf{e}^{-\mathbf{1}}) &= 0 \end{aligned}$$

and

$$\bar{\rho}\mathrm{tr}(\dot{\mathbf{F}}_\mathbf{g}\mathbf{F}_\mathbf{g}^{-\mathbf{1}}) = rJ_e \Rightarrow \rho\mathrm{tr}(\dot{\mathbf{F}}_\mathbf{g}\mathbf{F}_\mathbf{g}^{-\mathbf{1}}) = r \tag{2.11}$$

This final relation between the mass addition rate and the growth part of the deformation gradient tensor puts constraints on the growth with time.

2.2.3 Balance of Momentum

The linear momentum balance states that the rate of change of linear momentum $\frac{D}{Dt}\int_V \rho\mathbf{v}dV$ with time is equal to the net force on the body. Here, the change in momentum is due to the applied tractions, the body force and the change in mass due to tissue growth (cell proliferation). This can be written as:

$$\frac{D}{Dt}\int_V \rho\mathbf{v}dV = \int_S \mathbf{t}dS + \int_V \rho\mathbf{b}dV + \int_V r^g\mathbf{v}dV \tag{2.12}$$

Using the results from mass balance, we get

$$\frac{D}{Dt}\int_V \rho\mathbf{v}dV = \int_V \left(r^g\mathbf{v} + \rho\frac{D\mathbf{v}}{Dt}\right)dV \tag{2.13}$$

From the above two equations, we get

$$\int_V \left(r^g\mathbf{v} + \rho\frac{D\mathbf{v}}{Dt}\right)dV = \int_S \mathbf{t}dS + \int_V \rho\mathbf{b}dV + \int_V r^g\mathbf{v}dV$$

$$\Rightarrow \int_V \rho \frac{D\mathbf{v}}{Dt} dV = \int_S \mathbf{t} dS + \int_V \rho \mathbf{b} dV \tag{2.14}$$

We can apply divergence theorem on the traction surface integral to convert it to a volume integral in terms of the stress σ, using the relation

$$t_i = \sigma_{ij} n_j$$

$$\int_V \rho \frac{D\mathbf{v}}{Dt} dV = \int_V \left(\nabla \cdot \sigma + \rho \mathbf{b} \right) dV \tag{2.15}$$

Using the localisation argument, the equation is true for every volume element in the current configuration, the integrands must be equal.

$$\rho \frac{D\mathbf{v}}{Dt} = \nabla \cdot \sigma + \rho \mathbf{b} \tag{2.16}$$

The above equation in terms of the stresses generated in the tissue does not have a growth term. This means that tissue growth is not leading to stress. Instead the stresses are only due to elastic deformation. The LHS and the body force term are typically negligible as compared to the stress term on the RHS and can be approximated to zero. The equilibrium equation therefore becomes:

$$\nabla \cdot \sigma = \mathbf{0} \tag{2.17}$$

Similar to the equation for balance of linear momentum, we have the expression for change in angular momentum due to applied tractions, body force and tissue growth.

$$\frac{D}{Dt} \int_V \mathbf{r} \times \rho \mathbf{v} dV = \int_S \mathbf{r} \times \mathbf{t} dS + \int_V \mathbf{r} \times \rho \mathbf{b} dV + \int_V \mathbf{r} \times r^g \mathbf{v} dV \tag{2.18}$$

Using mass balance, we get

$$\frac{D}{Dt} \int_V \mathbf{r} \times \rho \mathbf{v} dV = \int_V \left(\mathbf{r} \times r^g \mathbf{v} + \rho \frac{D(\mathbf{r} \times \mathbf{v})}{Dt} \right) dV \tag{2.19}$$

From the above equations we get

$$\int_V \left(\mathbf{r} \times r^g \mathbf{v} + \rho \frac{D(\mathbf{r} \times \mathbf{v})}{Dt} \right) dV = \int_S \mathbf{r} \times \mathbf{t} dS + \int_V \mathbf{r} \times \rho \mathbf{b} dV + \int_V \mathbf{r} \times r^g \mathbf{v} dV$$

$$\Rightarrow \int_V \rho \frac{D(\mathbf{r} \times \mathbf{v})}{Dt} dV = \int_S \mathbf{r} \times \mathbf{t} dS + \int_V \mathbf{r} \times \rho \mathbf{b} dV \tag{2.20}$$

Applying divergence theorem on the traction surface integral to convert it to a volume integral in terms of the stress $\boldsymbol{\sigma}$, using the relation

$$t_i = \sigma_i j n_j$$

Equation 2.15 now becomes

$$\int_V \rho \frac{D(\mathbf{r} \times \mathbf{v})}{Dt} dV = \int_V \left(\nabla \cdot (\mathbf{r} \times \boldsymbol{\sigma}) + \rho \mathbf{b} \right) dV$$

$$\int_V \rho \frac{D(\mathbf{r} \times \mathbf{v})}{Dt} dV = \int_V \left((\nabla \cdot \mathbf{r}) \boldsymbol{\sigma} + \mathbf{r} \times (\nabla \cdot \boldsymbol{\sigma}) + \rho \mathbf{b} \right) dV \tag{2.21}$$

Using the localisation argument,

$$\rho \frac{D(\mathbf{r} \times \mathbf{v})}{Dt} = \left((\nabla \cdot \mathbf{r}) \boldsymbol{\sigma} + \mathbf{r} \times (\nabla \cdot \boldsymbol{\sigma}) + \rho \mathbf{b} \right) \tag{2.22}$$

Similar to linear momentum balance, the above equation in terms of the stresses generated in the tissue does not have a growth term. This means that tissue growth is not leading to stress, and the stresses are only due to elastic deformation. The LHS and the body force term are typically negligible as compared to the stress term on the RHS and can be approximated to zero. The divergence of stress is also zero from balance of linear momentum. The equilibrium equation therefore becomes:

$$\begin{aligned} (\nabla \cdot \mathbf{r}) \boldsymbol{\sigma} &= \mathbf{0} \\ \Rightarrow \epsilon_{ijk} r_{i,l} \sigma_{jl} &= 0 \\ \Rightarrow \epsilon_{ijk} \delta_{i,l} \sigma_{jl} &= 0 \\ \Rightarrow \epsilon_{ijk} \sigma_{ji} &= 0 \end{aligned}$$

For each $k = 1, 2, 3$, we get $\sigma_{ji} = \sigma ij$. So, σ is symmetric. That is,

$$\boldsymbol{\sigma} = \boldsymbol{\sigma}^T \tag{2.23}$$

2.3 Growth Part of Deformation Gradient

What form does growth take such that it satisfies these balance laws? Mass balance and cell number balance for density preserving growth caused by an increase in number of cells rather than mass of cells gave us the relation

$$\rho \mathrm{tr}(\dot{\mathbf{F}}_\mathbf{g}\mathbf{F}_\mathbf{g}^{-\mathbf{1}}) = r.$$

For isotropic growth, $\mathbf{F_g}$ will be such that the growwth in every direction is the same.

$$\mathbf{F_g} = \alpha(t)\bar{e}_i \otimes E_i \Rightarrow {\mathbf{F_g}}^{-1} = \frac{1}{\alpha(t)} E_i \otimes \bar{e}_i,$$

where $i = 1, 2, 3$.

The mass balance relation gives us

$$\rho tr\left(\frac{\dot{\alpha}(t)}{\alpha(t)}\bar{e}_i \otimes \bar{e}_i\right) = r \Rightarrow \frac{D\alpha(t)}{Dt} = \frac{3r}{\rho} = 3(k_d - k_a).$$

The growth stretch $\alpha(t)$ will therefore be of the form

$$\alpha(t) = Ce^{3(k_d - k_a)t}, \tag{2.24}$$

where C is the constant of integration and can take any value.

2.4 Elastic Stress Response

The elastic part of the deformation is assumed to follow hyperelastic theory.

We first define some strain measures and related quantities.The Green-Lagrange strain tensors associated with the deformation gradients $\mathbf{F_e}, \mathbf{F_g}$ and the total deformation gradient $\mathbf{F}$ are given as

$$\mathbf{E_e} = \tfrac{1}{2}\left(\mathbf{F_e^T F_e} - \mathbf{I}\right), \quad \mathbf{E_g} = \tfrac{1}{2}\left(\mathbf{F_g^T F_g} - \mathbf{I}\right), \quad \mathbf{E} = \tfrac{1}{2}\left(\mathbf{F^T F} - \mathbf{I}\right)$$

The velocity gradient tensor associated with the total deformation is given as

$$\mathbf{L} = \dot{\mathbf{F}}\mathbf{F}^{-1} = (\dot{\mathbf{F}}_\mathbf{e}\mathbf{F_g} + \mathbf{F_e}\dot{\mathbf{F}}_\mathbf{g})\mathbf{F_g}^{-1}\mathbf{F_e}^{-1} = \dot{\mathbf{F}}_\mathbf{e}\mathbf{F_e}^{-1} + \mathbf{F_e}\dot{\mathbf{F}}_\mathbf{g}\mathbf{F_g}^{-1}\mathbf{F_e}^{-1}$$

The first term is $\mathbf{L_e}$. Let the second term be $\mathbf{l_e}$ with its symmetric and asymmetric parts denoted by $\mathbf{d_e}$ and $\mathbf{w_e}$ respectively.

Let $\Psi(\mathbf{E_e}, \rho_g)$ be the strain energy per unit current mass. Since ρ_g^0 is the current mass per unit reference volume, the strain energy per unit volume is given as $\rho_g^0\Psi$.

The second Piola-Kirchoff stress can be obtained from the strain energy density function as follows from hyperelastic deformation theory

$$\mathbf{T} : d\mathbf{E} = \frac{\partial \rho_g^0 \Psi}{\partial \mathbf{E}} : d\mathbf{E}$$

or

$$\mathbf{T} = \frac{\partial \rho_g^0 \Psi}{\partial \mathbf{E}} \tag{2.25}$$

From the definition of the Green Lagrange strain tensors, we get the following relation between $\mathbf{E}$ and $\mathbf{E_e}$

$$\frac{\partial (E_e)_{ij}}{\partial E_{pq}} = (F_g^{-T})_{ik}\frac{\partial E_{kl}}{\partial E_{pq}}(F_g^{-1})_{lj} = (F_g^{-T})_{ik}\delta_{kp}\delta lq(F_g^{-1})_{lj} = (F_g^{-T})_{ip}(F_g^{-1})_{qj}$$
$$\Rightarrow T_{pq} = F_g^{-1})_{pi}\frac{\partial \rho_g^0 \Psi}{\partial E_{ij}}(F_g^{-T})_{jq}$$

which gives us

$$\mathbf{T} = \mathbf{F_g}^{-1}\frac{\partial \rho_g^0 \Psi}{\partial \mathbf{E_e}}\mathbf{F_g}^{-T} \tag{2.26}$$

The second P-K stress is related to the Kirchhoff stress $\boldsymbol{\tau}$ as

$$\mathbf{T} = \mathbf{F}^{-1}\boldsymbol{\tau}\mathbf{F}^{-T}$$

Using equation 2.26 we can get the expression for the Kirchhoff stress as

$\boldsymbol{\tau} = \mathbf{F}\mathbf{F_g}^{-1}\frac{\partial\rho_g^0\Psi}{\partial\mathbf{E_e}}\mathbf{F_g}^{-T}\mathbf{F}^T$

resulting in

$$\boldsymbol{\tau} = \mathbf{F_e}\frac{\partial\rho_g^0\Psi}{\partial\mathbf{E_e}}\mathbf{F_e}^T \tag{2.27}$$

This expression can be re-written in terms of the Cauchy-Green strain tensors as well.

$$\boldsymbol{\tau} = 2\mathbf{F_e}\frac{\partial\rho_g^0\Psi}{\partial\mathbf{C_e}}\mathbf{F_e}^T = 2\mathbf{F}\frac{\partial\rho_g^0\Psi}{\partial\mathbf{C}}\mathbf{F}^T \tag{2.28}$$

The Cauchy stress can be found from Kirchhoff stress as

$$\boldsymbol{\sigma} = \frac{2}{J}\mathbf{F_e}\frac{\partial\rho_g^0\Psi}{\partial\mathbf{C_e}}\mathbf{F_e}^T = \frac{1}{J}\mathbf{F_e}\frac{\partial\rho_g^0\Psi}{\partial\mathbf{E_e}}\mathbf{F_e}^T \tag{2.29}$$

We are considering isotropic elastic materials here, which is independent of the type of growth that is undergoes (isotropic or anisotropic). In order to take a strain energy density function that is compatible with incompressible elastic deformation without introducing an additional unknown coefficient, we take reduced forms of the elastic form of the deformation gradient using the transformation

$$\mathbf{F_e} = J_e^{\frac{1}{3}}\bar{\mathbf{F}}_\mathbf{e} \tag{2.30}$$

This transformation results in a decomposition of volume change and shape change, similar to the multiplicative decomposition described earlier - the change in volume being $J_e\mathbf{I}$ and the change in shape being $\bar{\mathbf{F}}_\mathbf{e}$. The strain energy per unit volume is of the form $W(\bar{I}_1, \bar{I}_2, J_e)$ where $\bar{I}_1, \bar{I}_2$ are the first and second invariant of $\bar{\mathbf{C}}_\mathbf{e}$ which has a similar definition.

$I_1 = \mathrm{tr}(\mathbf{C_e})$
$I_2 = \frac{1}{2}(I_1^2 - \mathrm{tr}(\mathbf{C_e}\mathbf{C_e}))$
$I_3 = \det(\mathbf{C_e}) = \det(\mathbf{F_e^T}\mathbf{F_e}) = J_e^2 \Rightarrow J_e = I_3^{\frac{1}{2}}$

$\bar{I}_1 = J_e^{-\frac{2}{3}} I_1 = I_3^{-\frac{1}{3}} I_1$
$\bar{I}_2 = J_e^{-\frac{4}{3}} I_2 = I_3^{-\frac{2}{3}} I_2$

We will need the following derivatives in order to find the Kirchhoff Stress.

$\frac{\partial I_1}{\partial C^e_{ij}} = \delta_{ij}, \frac{\partial I_2}{\partial C^e_{ij}} = -C^e_{ij} + I_1\delta_{ij}, \frac{\partial I_3}{\partial C^e_{ij}} = I_3 C^{e-T}_{ij}$

$\frac{\partial \bar{I}_1}{\partial C^e_{ij}} = \frac{\partial I_3^{-\frac{1}{3}}}{\partial C^e_{ij}} I_1 + I_3^{-\frac{1}{3}} \frac{\partial I_1}{\partial C^e_{ij}} = I_3^{-\frac{1}{3}}(-\frac{I_1}{3} C^{e-1}_{ij} + \delta_{ij})$

$\frac{\partial \bar{I}_2}{\partial C^e_{ij}} = \frac{\partial I_3^{-\frac{2}{3}}}{\partial C^e_{ij}} I_2 + I_3^{-\frac{2}{3}} \frac{\partial I_2}{\partial C^e_{ij}} = I_3^{-\frac{2}{3}}(-\frac{2I_2}{3} C^{e-1}_{ij} - C^e_{ij} + I_1\delta_{ij})$

$\frac{\partial \bar{J}_e}{\partial C^e_{ij}} = \frac{\partial I_3^{\frac{1}{2}}}{\partial C^e_{ij}} = \frac{1}{2} I_3^{\frac{1}{2}} C^{e-1}_{ij}$

We now calculate $\boldsymbol{\tau}$ and $\boldsymbol{\sigma}$ using these derivatives and chain rule.

$$\boldsymbol{\tau} = 2\mathbf{F_e}\frac{\partial W}{\partial \mathbf{C_e}}\mathbf{F_e}^T = 2\mathbf{F_e}\left(\frac{\partial W}{\partial \bar{I}_1}\frac{\partial \bar{I}_1}{\partial \mathbf{C_e}} + \frac{\partial W}{\partial \bar{I}_2}\frac{\partial \bar{I}_2}{\partial \mathbf{C_e}}\right) + \frac{\partial W}{\partial J_e}\frac{\partial J_e}{\partial \mathbf{C_e}}\mathbf{F_e}^T$$

$\Rightarrow \tau_{mn} = 2(-\frac{1}{3}\frac{\partial W}{\partial \bar{I}_1} J_e^{-\frac{2}{3}} I_1 - \frac{2}{3}\frac{\partial W}{\partial J_e} J_e^{-\frac{4}{3}} I_2 + \frac{1}{2}\frac{\partial W}{\partial J_e}) F^e_{mi}(F^e_{ip})^{-1}(F^e_{pj})^{-T} F^{eT}_{ip} + 2(\frac{\partial W}{\partial \bar{I}_1} J_e^{-\frac{2}{3}} + I_1 \frac{\partial W}{\partial \bar{I}_2} J_e^{-\frac{4}{3}}) F^e_{mi}\delta_{ij} F^{eT}_{jn} - 2\frac{\partial W}{\partial \bar{I}_2} J_e^{-\frac{4}{3}} F^e_{mi} F^{eT}_{ip} F^e_{pj} F^{eT}_{ip}$

$$\Rightarrow \boldsymbol{\tau} = 2\left[\left(\frac{\partial W}{\partial \bar{I}_1} + \bar{I}_1\frac{\partial W}{\partial \bar{I}_2}\right)\bar{\mathbf{B}}_\mathbf{e} - \frac{\partial W}{\partial \bar{I}_2}\bar{\mathbf{B}}_\mathbf{e}\bar{\mathbf{B}}_\mathbf{e} - \frac{1}{3}\left(\bar{I}_1\frac{\partial W}{\partial \bar{I}_1} + 2\bar{I}_2\frac{\partial W}{\partial \bar{I}_2}\right)\mathbf{I}\right] - J_e\frac{\partial W}{\partial J_e}\mathbf{I}$$

The Cauchy stress can therefore be found as

$$\boldsymbol{\sigma} = \frac{2}{J}\left[\left(\frac{\partial W}{\partial \bar{I}_1} + \bar{I}_1\frac{\partial W}{\partial \bar{I}_2}\right)\bar{\mathbf{B}}_\mathbf{e} - \frac{\partial W}{\partial \bar{I}_2}\bar{\mathbf{B}}_\mathbf{e}\bar{\mathbf{B}}_\mathbf{e} - \frac{1}{3}\left(\bar{I}_1\frac{\partial W}{\partial \bar{I}_1} + 2\bar{I}_2\frac{\partial W}{\partial \bar{I}_2}\right)\mathbf{I}\right] - \frac{J_e}{J}\frac{\partial W}{\partial J_e}\mathbf{I} \quad (2.31)$$

2.5 Finite Element Implementation of the Continuum Model

The expression for stress obtained using hyperelastic theory needs to be implemented numerically. For this, we linearise it to get the tangent stiffness matrix for the finite element simulations. We do this through a UMAT which takes this $DDSDDE$ as one of the inputs. As we can see, the stress and therefore the $DDSDDE$ depends mainly on the

elastic part of the deformation $\bar{\mathbf{F}}_\mathbf{e}$. The finite element software ABAQUS uses this UMAT ftakes the geometric input from the input file or GUI, which gives the information about $\mathbf{F}$. The UMAT also containes the growth part of the deformation gradient, and calculates the elastic part using this available information.

In the following sections, we find the expression for the $DDSDDE$ from stresses and discuss how it is used in the UMAT.

2.5.1 Principal of Virtual Work

The virtual work for a solid undergoing deformation δu in the current configuration is

$$\delta W_{int} = \int_V \boldsymbol{\sigma} : \delta\boldsymbol{\epsilon} dV$$

where δW_{int} is the virtual change in internal energy due to the virtual deformation and $\delta\boldsymbol{\epsilon} = \frac{1}{2}(\frac{\partial\delta u}{\partial x} + \frac{\partial\delta u}{\partial x}^T)$.

We can write the cauchy stress as the sum of its hydrostatic and deviatoric parts as

$$\boldsymbol{\sigma} = \boldsymbol{\sigma}' + \boldsymbol{\sigma}_v = \boldsymbol{\sigma}' - p\mathbf{I}$$

where $p = \frac{1}{3}tr(\boldsymbol{\sigma})$. The strain can also be decomposed as

$$\delta\boldsymbol{\epsilon} = \delta\boldsymbol{\epsilon}' + \frac{1}{3}\delta\epsilon_v\mathbf{I}$$

where $\delta\epsilon_v = tr(\boldsymbol{\epsilon})$

The virtual work equation now becomes

$\delta W_{int} = \int_V(\boldsymbol{\sigma}' - p\mathbf{I}) : (\delta\boldsymbol{\epsilon}' + \frac{1}{3}\delta\epsilon_v\mathbf{I})dV$
$= \int_V(\boldsymbol{\sigma}' : \delta\boldsymbol{\epsilon}' - p\mathbf{I} : \delta\boldsymbol{\epsilon}' + \boldsymbol{\sigma} : \frac{1}{3}\delta\epsilon_v\mathbf{I})dV$
$= \int_V(\boldsymbol{\sigma}' : \delta\boldsymbol{\epsilon}' - p(\mathbf{I} : \delta\boldsymbol{\epsilon} - \mathbf{I} : \frac{1}{3}\delta\epsilon_v\mathbf{I}) + \frac{1}{3}tr(\boldsymbol{\sigma})\delta\epsilon_v\mathbf{I})dV$
$= \int_V(\boldsymbol{\sigma}' : \delta\boldsymbol{\epsilon}' - p\delta\epsilon_v + p\delta\epsilon_v - p\delta\epsilon_v)dV$

So, we the virtual work equation finally is

$$\delta W_{int} = \int_V (\boldsymbol{\sigma}' : \delta\boldsymbol{\epsilon}' - p\delta\epsilon_v) dV = \int_{V_0} J(\boldsymbol{\sigma}' : \delta\boldsymbol{\epsilon}' - p\delta\epsilon_v) dV_0$$

We linearise the above equation as

$$D\delta W_{int} = \int_{V_0} \left(D(J\boldsymbol{\sigma}') : \delta\boldsymbol{\epsilon}' + J\boldsymbol{\sigma}' : D\delta\boldsymbol{\epsilon}' - D(Jp)\delta\epsilon_v - JpD(\delta\epsilon_v) \right) dV_0$$

2.5.2 Tangent Stiffness

This linearised form of virtual work is used in ABAQUS through a tangent stiffness matrix. The derivation for the form of the matrix used in the UMAT is given in Appendix A. The final expression is:

$$\begin{aligned} DDSDDE_{ijkl} &= \mathbb{C}^s_{ijpq}\delta_{pk}\delta_{ql} - \frac{1}{3}\mathbb{C}^s_{ijpq}\delta_{pq}\delta kl + \delta_{ij}Q_{kl} + Q_{ij}\delta_{kl} + K\delta_{ij}\delta_{kl} \\ &= \mathbb{C}^s_{ijkl} - \frac{1}{3}\mathbb{C}^s_{ijpp}\delta kl + \delta_{ij}Q_{kl} + Q_{ij}\delta_{kl} + K\delta_{ij}\delta_{kl} \end{aligned}$$

where

$$\begin{aligned} \mathbb{C}^s = {} & \frac{2}{J}\left(\frac{\partial W}{\partial \bar{I}_1} + \bar{I}_1\frac{\partial W}{\partial \bar{I}_2}\right)\mathbb{H}^1 - \frac{\partial W}{\partial \bar{I}_2}\mathbb{H}^2 + \frac{4}{J}\left(\frac{\partial^2 W}{\partial \bar{I}_1^2} + 2\bar{I}_1\frac{\partial^2 W}{\partial \bar{I}_1\partial \bar{I}_2} + \bar{I}_1^2\frac{\partial^2 W}{\partial \bar{I}_2^2}\right)\bar{\mathbf{B}}_\mathbf{e}\otimes\bar{\mathbf{B}}_\mathbf{e} \\ & - \frac{4}{J}\frac{\partial^2 W}{\partial \bar{I}_1\partial \bar{I}_2}(\bar{\mathbf{B}}_\mathbf{e}\otimes\bar{\mathbf{B}}_\mathbf{e}\cdot\bar{\mathbf{B}}_\mathbf{e} + \bar{\mathbf{B}}_\mathbf{e}\cdot\bar{\mathbf{B}}_\mathbf{e}\otimes\bar{\mathbf{B}}_\mathbf{e}) + \frac{4}{J}\frac{\partial^2 W}{\partial \bar{I}_2^2}\bar{\mathbf{B}}_\mathbf{e}\cdot\bar{\mathbf{B}}_\mathbf{e}\otimes\bar{\mathbf{B}}_\mathbf{e}\cdot\bar{\mathbf{B}}_\mathbf{e} \\ & - \frac{4}{3J}\left[\frac{\partial W}{\partial \bar{I}_1} + 2\bar{I}_1\frac{\partial W}{\partial \bar{I}_2} + \bar{I}_1^2\frac{\partial^2 W}{\partial \bar{I}_1^2} + (\bar{I}_1^2 + 2\bar{I}_2)\frac{\partial^2 W}{\partial \bar{I}_1\partial \bar{I}_2} + 2\bar{I}_1\bar{I}_2\frac{\partial^2 W}{\partial \bar{I}_2^2}\right](\mathbf{I}\otimes\bar{\mathbf{B}}_\mathbf{e} + \bar{\mathbf{B}}_\mathbf{e}\otimes\mathbf{I}) \\ & + \frac{4}{3J}\left(2\frac{\partial W}{\partial \bar{I}_1} + 2\bar{I}_1\frac{\partial^2 W}{\partial \bar{I}_1\partial \bar{I}_2} + 2\bar{I}_2\frac{\partial^2 W}{\partial \bar{I}_2^2}\right)(\mathbf{I}\otimes\bar{\mathbf{B}}_\mathbf{e}\cdot\bar{\mathbf{B}}_\mathbf{e} + \bar{\mathbf{B}}_\mathbf{e}\cdot\bar{\mathbf{B}}_\mathbf{e}\otimes\mathbf{I}) \end{aligned}$$

$$\mathbf{Q} = 2\left(\frac{\partial^2 W}{\partial \bar{I}_1\partial J_e} + \bar{I}_1\frac{\partial^2 W}{\partial \bar{I}_2\partial J_e}\right)\bar{\mathbf{B}}_\mathbf{e} - 2\frac{\partial^2 W}{\partial \bar{I}_2\partial J_e}\bar{\mathbf{B}}_\mathbf{e}\cdot\bar{\mathbf{B}}_\mathbf{e} - \frac{2}{3}\left(\bar{I}_1\frac{\partial^2 W}{\partial \bar{I}_1\partial J_e} + 2\bar{I}_2\frac{\partial^2 W}{\partial \bar{I}_2\partial J_e}\right)\mathbf{I}$$

$$K = J_e\frac{\partial^2 W}{\partial J_e^2} + \frac{\partial W}{\partial J_e}$$

Chapter 3

Growth and Deformation of Simple 3D Geometries

3.1 Growth within Fixed Surface Geometries

We first consider the case of thick, compressible cylindrical and spherical shells with all surfaces fixed. Constrained isotropic growth leads to the development of residual stresses within the sphere, which we can calculate analytically.

3.1.1 Fixed Cylindrical Shell

Analytical Solution

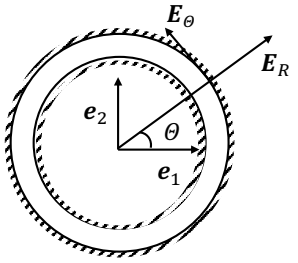

FIGURE 3.1: Schematic of cross section of growing cylindrical shell fixed at both surfaces

The growth part of the deformation gradient can be found between the reference and intermediate configurations in cylindrical coordinates.

$$\mathbf{F_g} = \nabla_0 \bar{\mathbf{x}} = \left(\mathbf{E}_R \frac{\partial}{\partial R} + \mathbf{E}_\Theta \frac{1}{R} \frac{\partial}{\partial \Theta} + \mathbf{E}_Z \frac{\partial}{\partial Z} \right) (\bar{r}\bar{\mathbf{e}}_r + \bar{z}\bar{\mathbf{e}}_z)$$

On simplification we get

$$\mathbf{F_g} = \frac{\partial \bar{r}}{\partial R}\bar{\mathbf{e}}_r \otimes \mathbf{E}_R + \frac{1}{R}\frac{\partial \bar{r}}{\partial \Theta}\bar{\mathbf{e}}_r \otimes \mathbf{E}_\Theta + \frac{\partial \bar{r}}{\partial Z}\bar{\mathbf{e}}_r \otimes \mathbf{E}_Z + \frac{\bar{r}}{R}\bar{\mathbf{e}}_\theta \otimes \mathbf{E}_\Theta + \frac{\partial \bar{z}}{\partial R}\bar{\mathbf{e}}_z \otimes \mathbf{E}_R + \frac{\partial \bar{z}}{\partial \Theta}\bar{\mathbf{e}}_z \otimes \mathbf{E}_\Theta + \frac{\partial \bar{z}}{\partial Z}\bar{\mathbf{e}}_z \otimes \mathbf{E}_Z \tag{3.1}$$

Since we are considering isotropic growth with growth stretch, say, $\alpha(t)$, $\mathbf{F_g}$ can also be written as

$$\mathbf{F_g} = \alpha(t)(\bar{\mathbf{e}}_r \otimes \mathbf{E}_R + \bar{\mathbf{e}}_\theta \otimes \mathbf{E}_\Theta + \bar{\mathbf{e}}_z \otimes \mathbf{E}_Z) \tag{3.2}$$

On comparing the two equations we get

$$\frac{1}{R}\frac{\partial \bar{r}}{\partial \Theta} = 0, \frac{\partial \bar{r}}{\partial Z} = 0 \Rightarrow \bar{r} = f(R)$$

Similarly, $\bar{z} = g(Z)$.

$$\frac{\partial \bar{r}}{\partial R} = \alpha = \frac{r}{R} \Rightarrow \bar{r} = f(R) = \alpha R$$

$$\frac{\partial \bar{z}}{\partial Z} = \alpha \Rightarrow \bar{z} = g(Z) = \alpha Z$$

Since the cylinder is completely fixed, the total deformation gradient between the current and the reference configurations is

$$\mathbf{F} = \mathbf{e}_r \otimes \mathbf{E}_R + \mathbf{e}_\theta \otimes \mathbf{E}_\Theta + \mathbf{e}_z \otimes \mathbf{E}_Z$$

We can get $\mathbf{F_e}$ as

$$\mathbf{F_e} = \mathbf{F}\mathbf{F_g}^{-1} = \frac{1}{\alpha}(\mathbf{e}_r \otimes \bar{\mathbf{e}}_r + \mathbf{e}_\theta \otimes \bar{\mathbf{e}}_\Theta + \mathbf{e}_z \otimes \bar{\mathbf{e}}_z)$$

$$\mathbf{B_e} = \mathbf{F_e}\mathbf{F_e}^T = \frac{1}{\alpha^2}(\mathbf{e}_r \otimes \mathbf{e}_r + \mathbf{e}_\theta \otimes \mathbf{e}_\theta + \mathbf{e}_z \otimes \mathbf{e}_z)$$

$J_e = \det(\mathbf{F_e}) = \frac{1}{\alpha^3}$
$\bar{\mathbf{B}}_\mathbf{e} = J_e^{-\frac{2}{3}} = \alpha^2 \mathbf{B_e} = \mathbf{I}$
$\bar{I}_1 = \mathrm{tr}(\bar{\mathbf{B}}_\mathbf{e}) = 3$

We use the following strain energy density function for compressible Neo-Hookean materials

$$W = C_{10}(\bar{I}_1 - 3) + \frac{1}{D_1}(J_e - 1)^2$$

Using the expression for Cauchy Stress we finally get the stresses as

$$\boldsymbol{\sigma} = \frac{2}{J}\left[C_{10}\bar{\mathbf{B}}_\mathbf{e} - \frac{\bar{I}_1}{3}C_{10}\mathbf{I}\right] + \frac{J_e}{J}\frac{2}{D_1}(J_e - 1)\mathbf{I} = \frac{2}{D_1}\frac{1}{\alpha^3}(\frac{1}{\alpha^3} - 1)\mathbf{I}$$

Numerical Solution for Linear Growth Stretch

We have shown before that for density preserving growth, we need to have the growth stretch to be exponential. Any other form would not preserve density for the isotropic case. We are first considering a linear growth stretch and then exponential.

The simulations were run with the material constants $C_{10} = 110$ and $D_1 = 0.001$. Since $C_{10} = \frac{\mu}{2}, D_1 = \frac{2}{\lambda}$ and Poisson's ratio is given as $\nu = \frac{\lambda}{2(\lambda + \mu)}$ it gives the poisson's ratio $\nu = 0.4505$ which indicates a compressible material. The growth stretch alpha was taken to be linearly dependent on time as

$\alpha(t) = 1 + (k_d - k_a)t$

where $k_d = 0.001$ and $k_a = 0$. The radial and tangential stresses σ_{rr} and $\sigma_{\theta\theta}$ obtained from the analytical and numerical methods match quite well as we can see from the plots below (Figure 3.2).

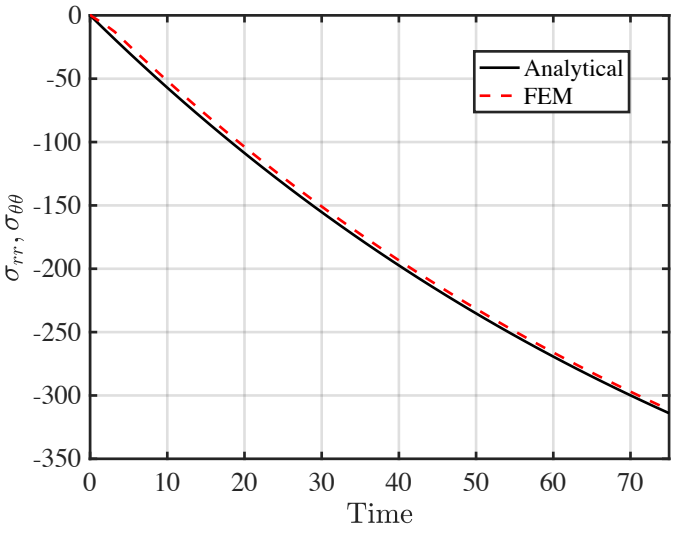

FIGURE 3.2: Comparison of Stress components VS Time obtained analytically and using FEM for the fixed cylinder problem with Linear Growth Stretch.$C_{10} = 110\ Pa$, $D_1 = 0.001\ Pa^{-1}$ and growth stretch is of the form $\alpha(t) = 1 + 0.5t$

Numerical Solution for Exponential Growth Stretch

We now consider the case of density preserving growth. We ran the simulations with the same parameters as above, except that the growth stretch is now of the form

$$\alpha(t) = e^{(k_d - k_a)t}$$

The numerical results match well with the analytical results (Figure 3.3).

When we compare the numerical results obtained from the linear and exponential case (Figure 3.5), we see that they are close. This makes sense since the exponential curve behaves close to a straight line at low values.

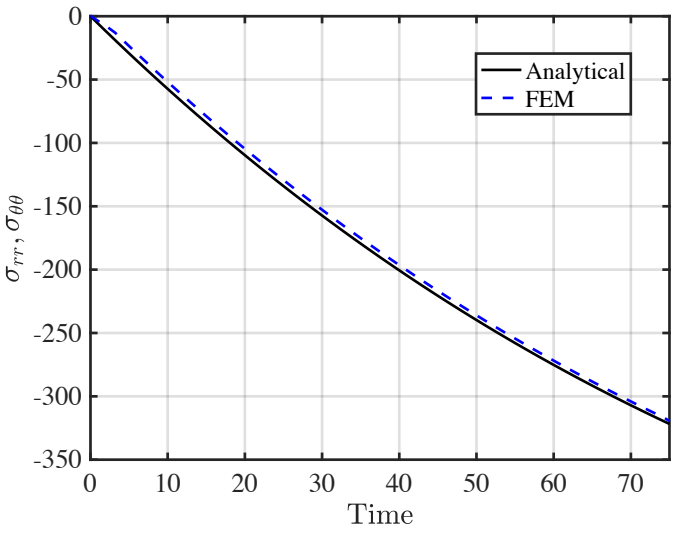

FIGURE 3.3: Comparison of Stress components VS Time obtained analytically and using FEM for the fixed cylinder problem with Exponential Growth Stretch.$C_{10} = 110\ Pa$, $D_1 = 0.001\ Pa^{-1}$ and growth stretch is of the form $\alpha(t) = e^{0.001t}$

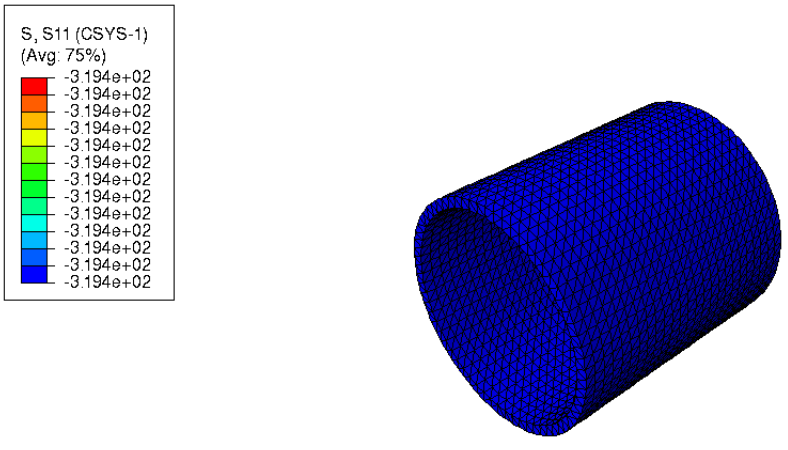

FIGURE 3.4: Deformed configuration of fixed cylinder showing Radial and Tangential stress distribution for exponential growth. C3D10H elements.

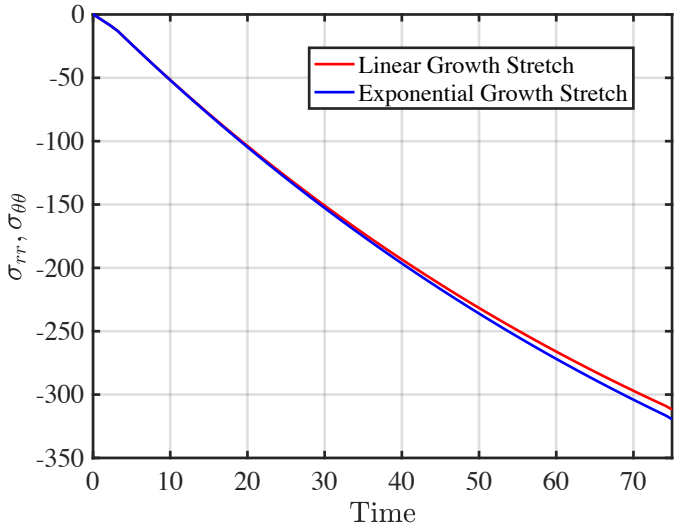

FIGURE 3.5: Comparison of Stress components VS Time obtained analytically for the fixed cylinder problem with Linear and Exponential Growth Stretch.

3.1.2 Fixed Spherical Shell

Analytical Solution

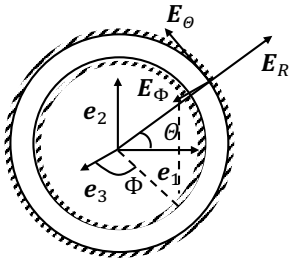

FIGURE 3.6: Schematic of cross section of growing spherical shell fixed at both surfaces

The growth part of the deformation gradient can be found between the reference and intermediate configurations in spherical coordinates similar to before.

$$\mathbf{F_g} = \nabla_0 \bar{\mathbf{x}} = \left(\mathbf{E}_R \frac{\partial}{\partial R} + \mathbf{E}_\Theta \frac{1}{R} \frac{\partial}{\partial \Theta} + \mathbf{E}_\Phi \frac{1}{R sin\Theta} \frac{\partial}{\partial \Phi} \right) (\bar{r} \bar{\mathbf{e}}_r)$$

On simplification and comparison with the isotropic $\mathbf{F_g}$ similar to the cylindrical case, we get $\bar{r} = f(R)$ and

$$\mathbf{F_g} = \alpha(t)(\bar{\mathbf{e}}_r \otimes \mathbf{E}_R + \bar{\mathbf{e}}_\theta \otimes \mathbf{E}_\Theta + \bar{\mathbf{e}}_\phi \otimes \mathbf{E}_\Phi)$$

$$(\frac{\partial \bar{r}}{\partial R})^2 = \alpha^2 = \frac{r^2}{R^2} \Rightarrow \bar{r} = f(R) = \alpha R.$$

Since the sphere is completely fixed, the total deformation gradient between the current and the reference configurations is

$$\mathbf{F} = \mathbf{e}_r \otimes \mathbf{E}_R + \mathbf{e}_\theta \otimes \mathbf{E}_\Theta + \mathbf{e}_\phi \otimes \mathbf{E}_\Phi.$$

We can get $\mathbf{F_e}$ as

$$\mathbf{F_e} = \mathbf{F}\mathbf{F_g}^{-1} = \frac{1}{\alpha}(\mathbf{e}_r \otimes \bar{\mathbf{e}}_r + \mathbf{e}_\theta \otimes \bar{\mathbf{e}}_\Theta + \mathbf{e}_\phi \otimes \bar{\mathbf{e}}_\Phi).$$

$$\mathbf{B_e} = \mathbf{F_e}\mathbf{F_e}^T = \frac{1}{\alpha^2}(\mathbf{e}_r \otimes \mathbf{e}_r + \mathbf{e}_\theta \otimes \mathbf{e}_\theta + \mathbf{e}_\phi \otimes \mathbf{e}_\phi)$$

$J_e = det(\mathbf{F_e}) = \frac{1}{\alpha^3}$
$\bar{\mathbf{B}}_\mathbf{e} = J_e^{-\frac{2}{3}} = \alpha^2 \mathbf{B_e} = \mathbf{I}$
$\bar{I}_1 = tr(\bar{\mathbf{B}}_\mathbf{e}) = 3$

We use the following strain energy density function for compressible Neo-Hookean materials

$$W = C_{10}(\bar{I}_1 - 3) + \frac{1}{D_1}(J_e - 1)^2.$$

Using the expression for Cauchy Stress

$$\boldsymbol{\sigma} = \frac{2}{J}\left[C_{10}\bar{\mathbf{B}}_\mathbf{e} - \frac{\bar{I}_1}{3}C_{10}\mathbf{I}\right] + \frac{J_e}{J}\frac{2}{D_1}(J_e - 1)\mathbf{I} = \frac{2}{D_1}\frac{1}{\alpha^3}(\frac{1}{\alpha^3} - 1)\mathbf{I}.$$

The stresses are the same as the cylindrical case. The only difference is that the stress components are in a different coordinate system.

Numerical Solution for Linear Growth Stretch

Simulations run for the same parameters and forms of growth stretch as in the cylindrical case. The analytical and FEM results match quite well as shown in Fig 3.7.

Numerical Solution for Exponential Growth Stretch

Again, same parameters and form of growth stretch as the cylindrical case. Results match well, as shown in Fig 3.8. The deformed configuration and stress distribution is shown in Fig 3.9.

When we compare the numerical results obtained from the linear and exponential case, we see in Fig 3.10 that they are close. This makes sense since the exponential curve behaves close to a straight line at low values.

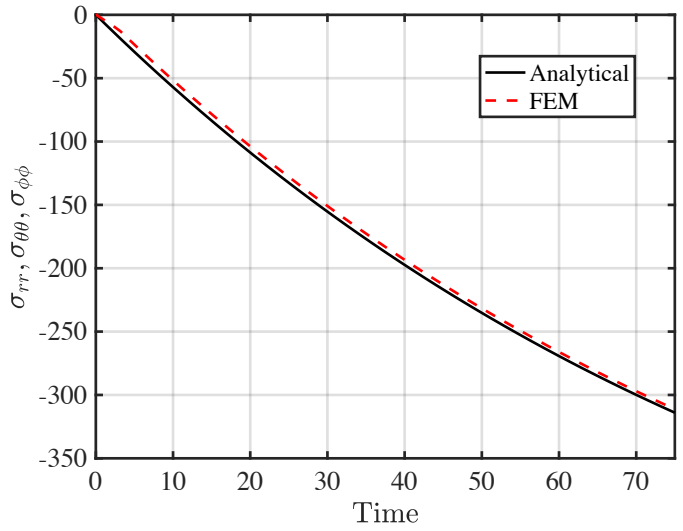

FIGURE 3.7: Comparison of Stress components VS Time obtained analytically and using FEM for the fixed sphere problem with Linear Growth Stretch.$C_{10} = 110\ Pa$, $D_1 = 0.001\ Pa^{-1}$ and growth stretch is of the form $\alpha(t) = 1 + 0.5t$

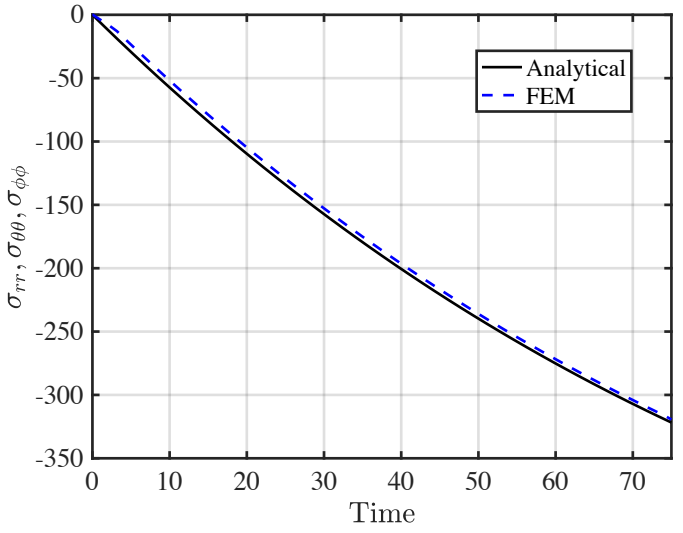

FIGURE 3.8: Comparison of Stress components VS Time obtained analytically and using FEM for the fixed sphere problem with Exponential Growth Stretch.$C_{10} = 110\ Pa$, $D_1 = 0.001\ Pa^{-1}$ and growth stretch is of the form $\alpha(t) = e^{0.001t}$

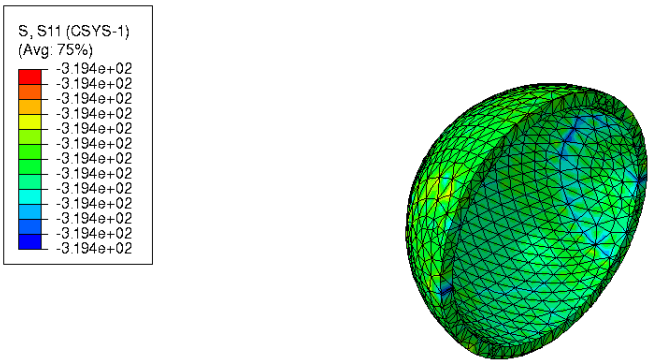

FIGURE 3.9: Deformed configuration of fixed cylinder showing Radial and Tangential stress distribution for exponential growth

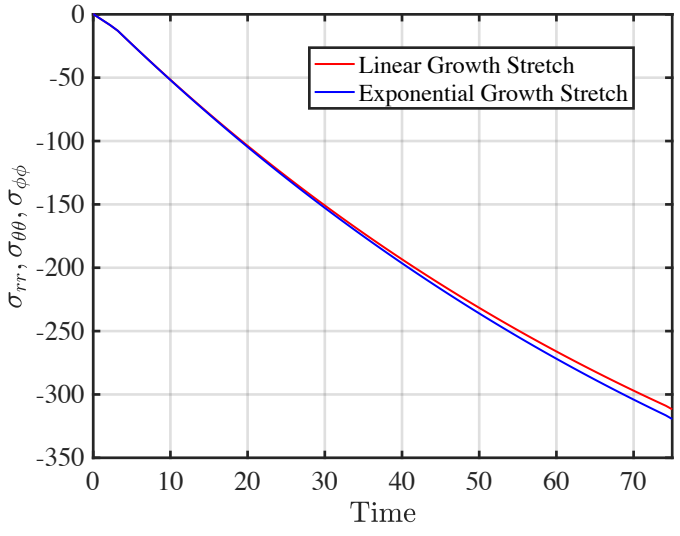

FIGURE 3.10: Comparison of Stress components VS Time obtained analytically for the fixed sphere problem with Linear and Exponential Growth Stretch. C3D10H elements.

3.2 Growth within Partially Fixed Surfaces

We now consider isotropic growth of thick, incompressible cylindrical and spherical shells with only the inner surface free and the rest of the surfaces fixed. The restricted growth is expected to cause an increase in the thickness of the shells.

3.2.1 Cylindrical Shell with Outer Surface Fixed

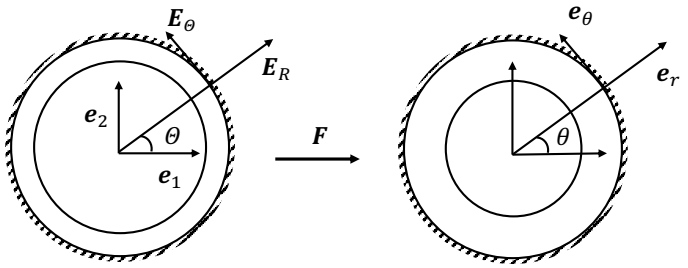

FIGURE 3.11: Schematic of the 2D cross section of reference and deformed configurations for cylindrical shell with outer surface fixed

Analytical Solution

We consider a modification to the fixed cylinder problem - with the outer surface fixed and inner surface traction free and growth restricted in the axial direction. This makes the problem equivalent to a 2D problem.

Since we are considering isotropic growth, we get

$$\mathbf{F_g} = \alpha(t)(\bar{\mathbf{e}}_r \otimes \mathbf{E}_R + \bar{\mathbf{e}}_\theta \otimes \mathbf{E}_\Theta) \tag{3.3}$$

The total deformation gradient is

$$\mathbf{F} = \frac{\partial r}{\partial R}\mathbf{e}_r \otimes \mathbf{E}_R + \frac{r}{R}\mathbf{e}_\theta \otimes \mathbf{E}_\Theta \tag{3.4}$$

The elastic part of the deformation gradient can be found as

$$\begin{aligned}\mathbf{F_e} = \mathbf{F}\mathbf{F_g}^{-1} &= (\frac{\partial r}{\partial R}\mathbf{e}_r \otimes \mathbf{E}_R + \frac{r}{R}\mathbf{e}_\theta \otimes \mathbf{E}_\Theta)\frac{1}{\alpha}(\mathbf{E_R} \otimes \bar{\mathbf{e}}_r + \mathbf{E}_\Theta \otimes \bar{\mathbf{e}}_\theta) \\ &= \frac{1}{\alpha}\frac{\partial r}{\partial R}\mathbf{e}_r \otimes \bar{\mathbf{e}}_\mathbf{r} + \frac{1}{\alpha}\frac{r}{R}\mathbf{e}_\theta \otimes \bar{\mathbf{e}}_\theta\end{aligned} \tag{3.5}$$

Assuming incompressibility during elastic deformation, we get

$$\begin{aligned}&\det(\mathbf{F_e}) = 1 \\ &\Rightarrow \frac{1}{\alpha^2}\frac{r}{R}\frac{\partial r}{\partial R} = 1 \\ &\Rightarrow r^2 = \alpha^2 R^2 + C_1\end{aligned} \tag{3.6}$$

We can find the integration constant using the fact that the outer boundary is fixed - the outer radius does not change after deformation. So, at $R = b_0, r = f(R) = b_0$. This gives $C_1 = b_0^2(1 - \alpha^2)$.

So we get

$$r^2 = \alpha^2 R^2 + b_0^2(1 - \alpha^2) \tag{3.7}$$

We take the following strain energy function for incompressible Neo-Hookean materials in terms of principal stretches

$$W = C_{10}(\lambda_r^{e2} + \lambda_\theta^{e2} + \lambda_z^{e2} - 3) - p(\lambda_r^e \lambda_\theta^e \lambda_z^e - 1) \tag{3.8}$$

where we define

$$\hat{W} = C_{10}(\lambda_r^{e2} + \lambda_\theta^{e2} + \lambda_z^{e2} - 3)$$

The stresses can be found as

$$\begin{aligned}\sigma_{rr} &= \frac{1}{J}(\lambda_r^e \frac{\partial \hat{W}}{\partial \lambda_r^e} - p(r)) = \frac{1}{\alpha^2}(2C_{10}\lambda_r^{e2} - p(r)) \\ \sigma_{\theta\theta} &= \frac{1}{J}(\lambda_\theta^e \frac{\partial \hat{W}}{\partial \lambda_\theta^e} - p(r)) = \frac{1}{\alpha^2}(2C_{10}\lambda_\theta^{e2} - p(r))\end{aligned}$$

where the principal stretches are

$$\lambda_r^e = \frac{1}{\alpha}\frac{\partial r}{\partial R} \Rightarrow \lambda_r^{e2} = 1 - \frac{C_1}{r^2}$$
$$\lambda_\theta^e = \frac{1}{\alpha}\frac{r}{R} \Rightarrow \lambda_r^{e2} = \frac{1}{1-\frac{C_1}{r^2}}$$

The stresses must satisfy equilibrium.

$$\frac{\partial \sigma_{rr}}{\partial r} + \frac{\sigma_{rr} - \sigma_{\theta\theta}}{r} = 0$$

This equilibrium condition gives us $p(r)$ as

$$p(r) = 2C_{10}\left[\frac{4}{3}(1-\frac{C_1}{r^2})^{\frac{3}{2}} + \frac{1}{2}log(\frac{1}{1-\frac{C_1}{r^2}}) + \frac{1}{2}\frac{C_1}{r^2}\right] + C_2$$

To find the value of the integration constant C_2 we use the condition that the inner surface is traction free, i.e. $\sigma_{rr} = 0$ for $r = 0$.

$$C_2 = 2C_{10}\left[1 - \frac{C_1}{a^2} - \frac{4}{3}(1-\frac{C_1}{a^2})^{\frac{3}{2}} - \frac{1}{2}log(\frac{1}{1-\frac{C_1}{a^2}}) - \frac{1}{2}\frac{C_1}{a^2}\right]$$

The stresses finally become

$$\sigma_{rr} = \frac{2C_{10}}{\alpha^2}\left(1 - \frac{C_1}{r^2} - \left[\frac{4}{3}(1-\frac{C_1}{r^2})^{\frac{3}{2}} + \frac{1}{2}log(\frac{1}{1-\frac{C_1}{r^2}}) + \frac{1}{2}\frac{C_1}{r^2}\right]\right)$$
$$- \frac{2C_{10}}{\alpha^2}\left(1 - \frac{C_1}{a^2} - \frac{4}{3}(1-\frac{C_1}{a^2})^{\frac{3}{2}} - \frac{1}{2}log(\frac{1}{1-\frac{C_1}{a^2}}) - \frac{1}{2}\frac{C_1}{a^2}\right)$$
$$\sigma_{\theta\theta} = \frac{2C_{10}}{\alpha^2}\left(\frac{1}{1-\frac{C_1}{r^2}} - \left[\frac{4}{3}(1-\frac{C_1}{r^2})^{\frac{3}{2}} + \frac{1}{2}log(\frac{1}{1-\frac{C_1}{r^2}}) + \frac{1}{2}\frac{C_1}{r^2}\right]\right)$$
$$- \frac{2C_{10}}{\alpha^2}\left(1 - \frac{C_1}{a^2} - \frac{4}{3}(1-\frac{C_1}{a^2})^{\frac{3}{2}} - \frac{1}{2}log(\frac{1}{1-\frac{C_1}{a^2}}) - \frac{1}{2}\frac{C_1}{a^2}\right)$$

Numerical Solution

For incompressibility, we used the parameter values $C_{10} = 110$ and $D_1 = 10^{-8}$ which gives Poisson's ratio close to 0.5.

The calculated radial stresses are almost zero and the FEM radial stresses are between zero and -3 to -4. They match relatively well. The analytical and FEM tangential stresses however follow a similar trend across the thickness but are shifted in values. This is also seen in the case of sphere (next section).

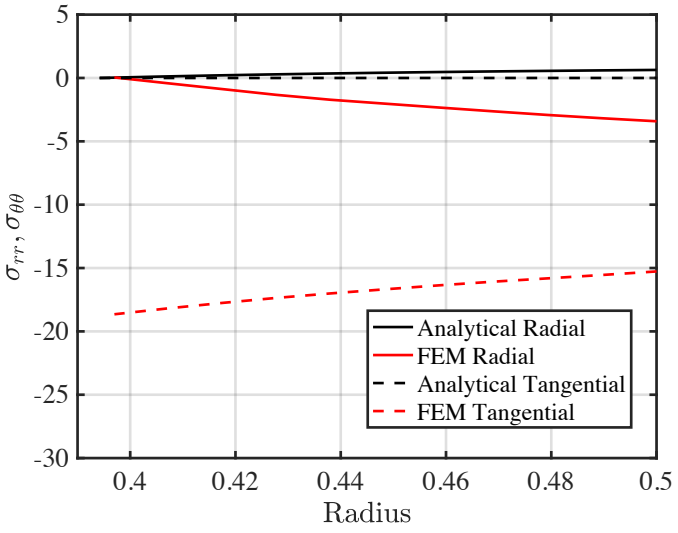

FIGURE 3.12: Comparison of Stress components across the radius obtained analytically and using FEM for a cylinder with outer surface fixed.$C_{10} = 110\ Pa$, $D_1 = 10^{-8}\ Pa^{-1}$ and growth stretch is of the form $\alpha(t) = e^{0.001t}$

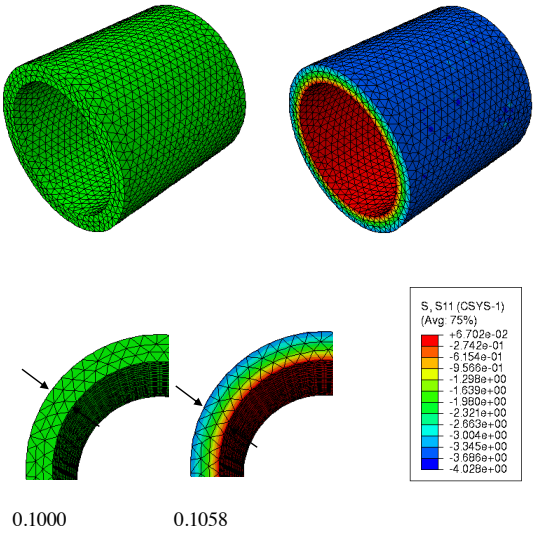

FIGURE 3.13: Deformed configuration of cylinder with outer surface fixed showing Radial Stress distribution and increased thickness (25 time steps)

3.2.2 Spherical Shell with Outer Surface Fixed

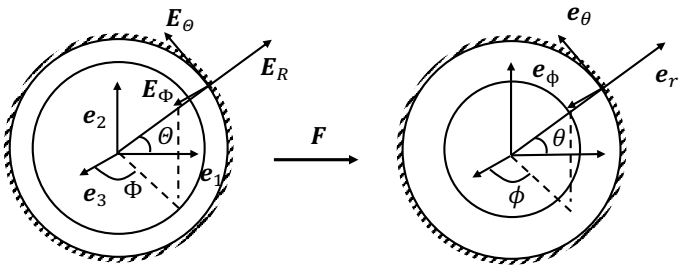

FIGURE 3.14: Schematic of the 2D cross section of reference and deformed configurations for spherical shell with outer surface fixed

Analytical Solution

We consider the case of a spherical shell with its outer surface fixed. We proceed similar to the cylinder, but unlike the cylinder this problem is a three dimensional problem.

Since we are considering isotropic growth, we get

$$\mathbf{F_g} = \alpha(t)(\bar{\mathbf{e}}_r \otimes \mathbf{E}_R + \bar{\mathbf{e}}_\theta \otimes \mathbf{E}_\Theta + \bar{\mathbf{e}}_\phi \otimes \mathbf{E}_\Phi) \tag{3.9}$$

The total deformation gradient is

$$\mathbf{F} = \frac{\partial r}{\partial R}\mathbf{e}_r \otimes \mathbf{E}_R + \frac{r}{R}\mathbf{e}_\theta \otimes \mathbf{E}_\Theta + \frac{r}{R}\mathbf{e}_\phi \otimes \mathbf{E}_\Phi \tag{3.10}$$

The elastic part of the deformation gradient can be found as

$$\begin{aligned}\mathbf{F_e} &= \mathbf{F}\mathbf{F_g}^{-1} \\ &= (\frac{\partial r}{\partial R}\mathbf{e}_r \otimes \mathbf{E}_R + \frac{r}{R}\mathbf{e}_\theta \otimes \mathbf{E}_\Theta + \frac{r}{R}\mathbf{e}_\phi \otimes \mathbf{E}_\Phi)\frac{1}{\alpha}(\bar{\mathbf{e}}_r \otimes \mathbf{E}_R + \bar{\mathbf{e}}_\theta \otimes \mathbf{E}_\Theta + \bar{\mathbf{e}}_\phi \otimes \mathbf{E}_\Phi) \\ &= \frac{1}{\alpha}\frac{\partial r}{\partial R}\mathbf{e}_r \otimes \bar{\mathbf{e}}_\mathbf{r} + \frac{1}{\alpha}\frac{r}{R}(\mathbf{e}_\theta \otimes \bar{\mathbf{e}}_\theta + \mathbf{e}_\phi \otimes \bar{\mathbf{e}}_\phi)\end{aligned} \tag{3.11}$$

Assuming incompressibility during elastic deformation, we get

$$\begin{aligned} &\det(\mathbf{F_e}) = 1 \\ &\Rightarrow \frac{1}{\alpha^3}\frac{r^2}{R^2}\frac{\partial r}{\partial R} = 1 \\ &\Rightarrow r^3 = \alpha^3 R^3 + C_1 \end{aligned} \tag{3.12}$$

We can find the integration constant using the fact that the outer boundary is fixed - the outer radius does not change after deformation. So, at $R = b_0, r = f(R) = b_0$. This gives $C_1 = b_0^3(1-\alpha^3)$.

So we get

$$r^3 = \alpha^3 R^3 + b_0^3(1-\alpha^3) \tag{3.13}$$

We take the following strain energy function for incompressible Neo-Hookean materials in terms of principal stretches

$$W = C_{10}(\lambda_r^{e2} + \lambda_\theta^{e2} + \lambda_z^{e2} - 3) - p(\lambda_r^e \lambda_\theta^e \lambda_z^e - 1) \tag{3.14}$$

where we define

$$\hat{W} = C_{10}(\lambda_r^{e2} + \lambda_\theta^{e2} + \lambda_z^{e2} - 3)$$

The stresses can be found as

$$\begin{aligned} \sigma_{rr} &= \frac{1}{J}(\lambda_r^e \frac{\partial \hat{W}}{\partial \lambda_r^e} - p(r)) = \frac{1}{\alpha^2}(2C_{10}\lambda_r^{e2} - p(r)) \\ \sigma_{\theta\theta} &= \frac{1}{J}(\lambda_\theta^e \frac{\partial \hat{W}}{\partial \lambda_\theta^e} - p(r)) = \frac{1}{\alpha^2}(2C_{10}\lambda_\theta^{e2} - p(r)) \end{aligned}$$

where the principal stretches are

$$\begin{aligned} \lambda_r^e &= \frac{1}{\alpha}\frac{\partial r}{\partial R} \Rightarrow \lambda_r^{e2} = \frac{1}{r^4}(r^3 - (1-\alpha^3)b_0^3)^{\frac{4}{3}} \\ \lambda_\theta^e &= \frac{1}{\alpha}\frac{r}{R} \Rightarrow \lambda_r^{e2} = \frac{r^2}{r^3 - (1-\alpha^3)b_0^3} \end{aligned}$$

The stresses must satisfy equilibrium.

$$\frac{\partial \sigma_{rr}}{\partial r} + \frac{2\sigma_{rr} - \sigma_{\theta\theta} - \sigma_{\phi\phi}}{r} = 0$$

This equilibrium condition gives us $p(r)$ as

$$p(r) = \frac{C_{10}}{\alpha r^4}(b_0^3(\alpha^3 - 1) + r^3)^{\frac{1}{3}}((\alpha^3 - 1)b_0^3 - 3r^3) + C_2$$

To find the value of the integration constant C_2 we use the condition that the inner surface is traction free, i.e. $\sigma_{rr} = 0$ for $r = 0$.

$$C_2 = \frac{C_{10}}{a^4} a_0 (2\alpha^3 a_0^3 - (\alpha^3 - 1)b_0^3 + 3a^3)$$

The stresses finally become

$$\begin{aligned}
\sigma_{rr} = {} & \frac{2C_{10}}{\alpha^2}\left(\frac{1}{r^4}(r^3 - (1-\alpha^3)b_0^3)^{\frac{4}{3}}\right) \\
& - \frac{C_{10}}{\alpha r^4}(b_0^3(\alpha^3 - 1) + r^3)^{\frac{1}{3}}((\alpha^3 - 1)b_0^3 - 3r^3) - \frac{C_{10}}{a^4} a_0 (2\alpha^3 a_0^3 - (\alpha^3 - 1)b_0^3 + 3a^3) \\
\sigma_{\theta\theta} = {} & \frac{2C_{10}}{\alpha^2}\left(\frac{r^2}{r^3 - (1-\alpha^3)b_0^3}\right) \\
& - \frac{C_{10}}{\alpha r^4}(b_0^3(\alpha^3 - 1) + r^3)^{\frac{1}{3}}((\alpha^3 - 1)b_0^3 - 3r^3) - \frac{C_{10}}{a^4} a_0 (2\alpha^3 a_0^3 - (\alpha^3 - 1)b_0^3 + 3a^3)
\end{aligned}$$

Numerical Solution

The analytical and FEM radial stresses are almost the same across thickness, as observed in the following Figure 3.15. The tangential stresses however, like in the cylinder case, follow the exact same trend across the thickness but are a bit shifted in values.

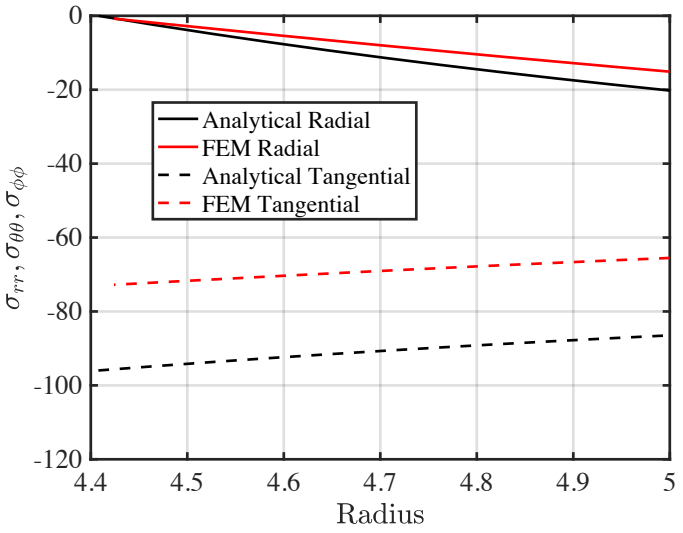

FIGURE 3.15: Comparison of Stress components across the radius obtained analytically and using FEM for a sphere with outer surface fixed.$C_{10} = 110\ Pa$, $D_1 = 10^{-8}\ Pa^{-1}$ and growth stretch is of the form $\alpha(t) = e^{0.001t}$

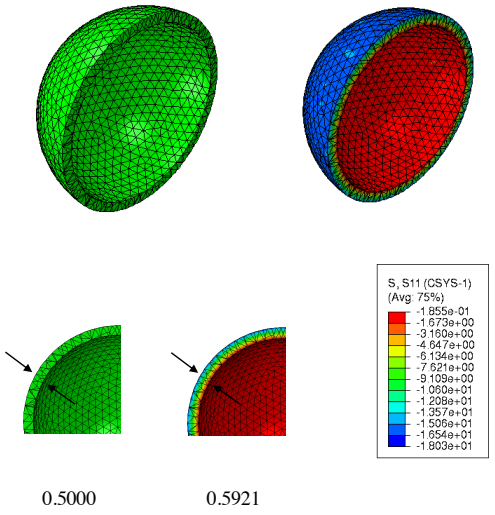

FIGURE 3.16: Deformed configuration of sphere with outer surface fixed showing Radial Stress distribution and increased thickness (50 time steps)

3.3 Conclusion

Our model can accurately calculate the displacements and hence the deformed configurations for compressible and incompressible 3D bodies undergoing growth. It can also predict the radial stresses that develop within the body fairly accurately. However, it shows some inaccuracy in the tangential stresses when it comes to incompressible materials. This inaccuracy in stresses in some incompressible cases could be because we have not used an iterative stress update in out UMAT. Instead we have used the expression for stresses that we derived for the compressible case along with a pseudo-incompressible scheme, i.e. a very small D_1. In the next chapter, we test whether our model can predict buckling due to growth.

Chapter 4

Growth and Buckling of Complex Geometries

We now move on to geometries for which we cannot find analytical solutions easily. We want to see if our model can correctly predict growth driven deformation for these scenarios.

4.1 Buckling of Circular Sheet

We consider a thin circular sheet of definite thickness and consider two cases of growth: only radial and only tangential. We expect that if there is only radial growth and the circumference is constrained to increase, the sheet will bulge out of plane into a hat like shape. And if there is tangential growth while all rigid body motions are fixed, we expect to see a rippled edge, or a saddle like shape.[3] These displacements can be quantified as

$$w(\rho, \theta) = \xi(\rho) cos(m\theta), [3]$$

where ρ is the ratio of the radial distance of the point and the initial radius of the circular sheet, w is the out of plane displacement at any point and ξ is some function of ρ. The different shapes that the sheet can deform into can be described by different values of the mode m.

Since we are considering anisotropic growth, the growth directions at any point matter. The growth tensor therefore needs to be transformed into the global coordinate system

from the principal coordinates. This makes the growth position dependent in the global coordinates.

4.1.1 The Hat

We first started with a flat circular sheet and fixed the circumference completely. We gave it a constant radial growth stretch of 1.0500. We saw that in plane stresses developed but there was no out of plane displacement. This prompted us to bias the sheet towards buckling, since our model does not account for it. We did this by introducing a very small out of plane bend in the sheet. With the same circumference fixed boundary condition and only a radial growth stretch, we obtained the buckled hat configuration, or mode $m = 0$ case.

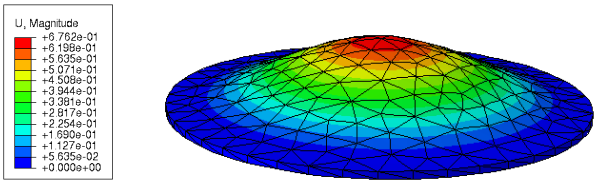

FIGURE 4.1: Displacements and the deformed hat shape ($m = 0$) for constant radial growth rate of 1.0500. Circumference of the sheet is completely fixed.

4.1.2 The Saddle

A flat circular sheet with only tangential growth and two points fixed to restrict rigid body motion only gave us residual stresses rather than out of plane displacement, like in the case of radial growth. We therefore needed to bias the sheet with an initial displacement field that varies according to mode $m = 2$ case. We did so through a user defined displacement boundary condition using the DISP subroutine, with $\xi = \dfrac{0.025}{R_{init}}$,.

The displacement subroutine ensures that rigid body modes are restricted and therefore doesn't need any other boundary conditions. When we applied a constant tangential growth, we saw an increase in the out of place displacement along the initial bias, giving the sheet a saddle shape.

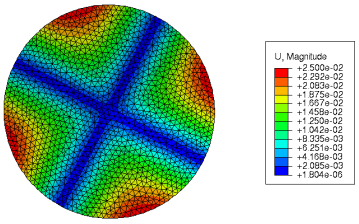

FIGURE 4.2: Initial displacement bias given towards a saddle shape

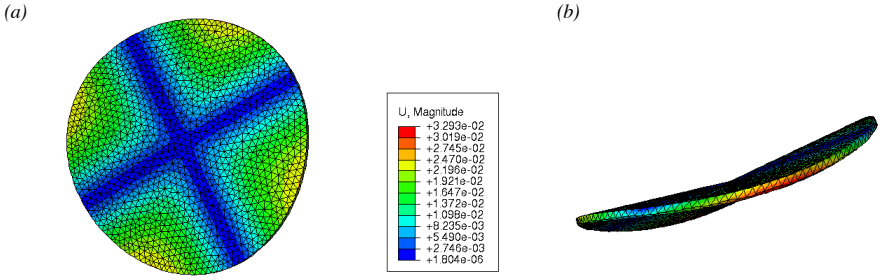

FIGURE 4.3: Displacements and the deformed saddle shape (Displacements scaled 20x), or $m = 2$, for constant tangential growth rate of 1.0500

When we used an exponentially time-varying growth stretch and hence imposing a density preserving growth, we saw a further increase in he out of plane displacement along the initial bias.

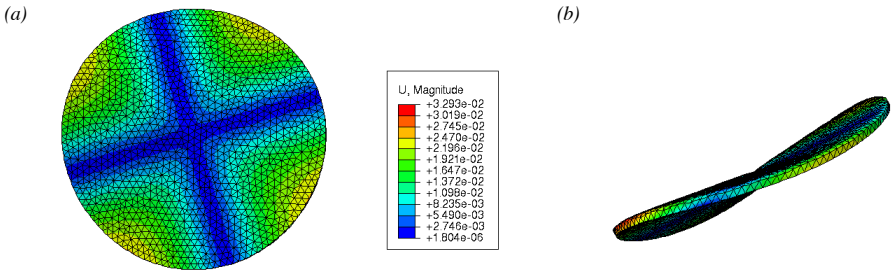

FIGURE 4.4: Displacements and the deformed saddle shape (Displacements scaled 20x), or $m = 2$, for exponential tangential growth rate of $e^{0.001t}$

4.2 Conclusion

Our UMAT does not lead to buckling of flat sheets despite restricted growth unless there is a bias towards buckling. When the aforementioned bias is present, the sheets buckle as expected from buckling models as shown by Dervaux and Amar (2008)[3].

Chapter 5

Conclusion

In this work, we have developed a numerical model that accurately describes the deformation caused by growth in ultra-soft tissues. To achieve this, we formulated the governing balance equations, and virtual work equation which was subsequently linearised for numerical implementation. Moreover, we created a UMAT designed for the finite element implementation on ABAQUS.

To evaluate the performance of our model, we conducted tests on various three-dimensional shapes and sheet-like geometries, considering both isotropic and anisotropic growth rates. Our model consistently generated the expected deformations across all cases. Additionally, it provided fairly accurate radial stress values, particularly for those cases that could be easily solved analytically.

5.1 Limitations and Future Directions

Our model lacks an iterative stress update, which may be the cause of inaccuracies in tangential stresses. Furthermore, when considering non-homogeneous cases, the UMAT currently requires growth rates and principal directions at every node within the body. These parameters are calculated based on the specific geometries employed in the model. However, in practical scenarios involving actual tissues, growth data can only be measured at finite points and must be interpolated across the body for the UMAT to function properly.

These limitations of the model point towards future directions for improvement and research. By addressing these limitations, the model can be enhanced and subsequently tested on geometries that closely resemble actual tissues.

Appendix A

Tangent Stiffness Matrix (DDSDDE)

Let us find each of the linearised terms separately first.

$$D\mathbf{F_e} = \nabla D\mathbf{u} = \mathbf{F_e}^T \nabla D\mathbf{u}$$

$$D\mathbf{L} = \frac{\partial D\mathbf{u}}{\partial \mathbf{x}} = \nabla D\mathbf{u}$$

$$D\boldsymbol{\epsilon} = \frac{1}{2}\left(D\mathbf{L} + (D\mathbf{L})^T\right)$$

$$DJ = J\text{tr}(\mathbf{F}^{-T}\mathbf{F}^T \nabla D\mathbf{u}) = J\text{tr}(\nabla D\mathbf{u})$$

Since the trace of a tensor is equal to the trace of the symmetric part of the tensor, we get

$$DJ = \frac{1}{2}J\text{tr}\left(D\mathbf{L} + (D\mathbf{L})^T\right) = J\text{tr}(\boldsymbol{\epsilon}) = JD\epsilon_v$$

Similarly,

$$DJ_e = J_e\text{tr}(\nabla D\mathbf{u}) = J_e D\epsilon_v$$

$$D\bar{\mathbf{F}}_\mathbf{e} = D(J_e^{-\frac{1}{3}}\mathbf{F_e}) = D(J_e^{-\frac{1}{3}})\mathbf{F_e} + J_e^{-\frac{1}{3}}D\mathbf{F_e} = -\frac{1}{3}D\epsilon_v\bar{\mathbf{F}}_\mathbf{e} + J_e^{-\frac{1}{3}}\nabla_g D\mathbf{u}$$

Using indicial notation to simplify the second term

$$\frac{\partial}{\partial x_i} = \frac{\partial \bar{x}_j}{\partial x_i}\frac{\partial}{\partial \bar{x}_j} \Rightarrow \nabla_i = F_{ji}^{e-1}(\nabla_g)_j = \nabla_j \Rightarrow (\nabla_g)_i DU_k = F_{ij}^{eT}\nabla Du_k = F_{ij}^{eT}DL_{kj}$$

So, we finally get

$$D\bar{\mathbf{F}}_\mathbf{e} = -\frac{1}{3}D\epsilon_v\bar{\mathbf{F}}_\mathbf{e} + D\mathbf{L}\bar{\mathbf{F}}_\mathbf{e}$$

Using this result we can get

$$\begin{aligned}
D\bar{\mathbf{B}}_\mathbf{e} &= D(\bar{\mathbf{F}}_\mathbf{e}\bar{\mathbf{F}}_\mathbf{e}^T) = D(\bar{\mathbf{F}}_\mathbf{e})\bar{\mathbf{F}}_\mathbf{e}^T + \bar{\mathbf{F}}_\mathbf{e}D(\bar{\mathbf{F}}_\mathbf{e}^T) \\
&= (-\frac{1}{3}D\epsilon_v\bar{\mathbf{F}}_\mathbf{e} + D\mathbf{L}\bar{\mathbf{F}}_\mathbf{e})\bar{\mathbf{F}}_\mathbf{e}^T + \bar{\mathbf{F}}_\mathbf{e}(-\frac{1}{3}D\epsilon_v\bar{\mathbf{F}}_\mathbf{e}^T + \bar{\mathbf{F}}_\mathbf{e}^T D\mathbf{L}^T) \\
&= -\frac{2}{3}D\epsilon_v + D\mathbf{L}\bar{\mathbf{B}}_\mathbf{e} + \bar{\mathbf{B}}_\mathbf{e}D\mathbf{L}^T \\
&= -\frac{2}{3}D\epsilon_v + \frac{1}{2}(D\mathbf{L} + D\mathbf{L}^T)\bar{\mathbf{B}}_\mathbf{e} + \frac{1}{2}(D\mathbf{L} - D\mathbf{L}^T)\bar{\mathbf{B}}_\mathbf{e} + \bar{\mathbf{B}}_\mathbf{e}\frac{1}{2}(D\mathbf{L}^T + D\mathbf{L})^T) + \bar{\mathbf{B}}_\mathbf{e}\frac{1}{2}(D\mathbf{L}^T - D\mathbf{L})^T) \\
&= -\frac{2}{3}D\epsilon_v + D\boldsymbol{\epsilon}\bar{\mathbf{B}}_\mathbf{e} + D\boldsymbol{\omega}\bar{\mathbf{B}}_\mathbf{e} + \bar{\mathbf{B}}_\mathbf{e}D\boldsymbol{\epsilon} - \bar{\mathbf{B}}_\mathbf{e}D\boldsymbol{\omega} \\
&= (D\boldsymbol{\epsilon} - \frac{1}{3}D\epsilon_v)\bar{\mathbf{B}}_\mathbf{e} + \bar{\mathbf{B}}_\mathbf{e}(D\boldsymbol{\epsilon} - \frac{1}{3}D\epsilon_v) + D\boldsymbol{\omega}\bar{\mathbf{B}}_\mathbf{e} - \bar{\mathbf{B}}_\mathbf{e}D\boldsymbol{\omega} \\
&= D\boldsymbol{\epsilon}'\bar{\mathbf{B}}_\mathbf{e} + \bar{\mathbf{B}}_\mathbf{e}D\boldsymbol{\epsilon}' + D\boldsymbol{\omega}\bar{\mathbf{B}}_\mathbf{e} - \bar{\mathbf{B}}_\mathbf{e}D\boldsymbol{\omega}
\end{aligned}$$

The first two terms can be written as

$$\begin{aligned}
D\epsilon'_{ip}\bar{B}^e_{pj} + \bar{B}^e_{ip}D\epsilon'_{pj} &= \frac{1}{2}(\delta_{ik}\bar{B}^e_{jl} + \delta_{jl}\bar{B}^e_{ik} + \delta_{il}\bar{B}^e_{jk} + \delta_{jk}\bar{B}^e_{il}) \\
&= \mathbb{H}^1_{ijkl}D\epsilon'_{kl}
\end{aligned}$$

Substituting this, we get

$$D\bar{\mathbf{B}}_\mathbf{e} = \mathbb{H}^\mathbf{1} : D\boldsymbol{\epsilon}' + D\boldsymbol{\omega}\bar{\mathbf{B}}_\mathbf{e} - \bar{\mathbf{B}}_\mathbf{e}D\boldsymbol{\omega}$$

Similarly,

$$\begin{aligned} D(\bar{\mathbf{B}}_\mathbf{e}\bar{\mathbf{B}}_\mathbf{e}) &= D(\bar{\mathbf{B}}_\mathbf{e})\bar{\mathbf{B}}_\mathbf{e} + \bar{\mathbf{B}}_\mathbf{e}D(\bar{\mathbf{B}}_\mathbf{e}) \\ &= (\mathbb{H}^\mathbf{1} : D\boldsymbol{\epsilon}' + D\boldsymbol{\omega}\bar{\mathbf{B}}_\mathbf{e} - \bar{\mathbf{B}}_\mathbf{e}D\boldsymbol{\omega})\bar{\mathbf{B}}_\mathbf{e} + \bar{\mathbf{B}}_\mathbf{e}(\mathbb{H}^\mathbf{1} : D\boldsymbol{\epsilon}' + D\boldsymbol{\omega}\bar{\mathbf{B}}_\mathbf{e} - \bar{\mathbf{B}}_\mathbf{e}D\boldsymbol{\omega}) \\ &= (\mathbb{H}^\mathbf{1} : D\boldsymbol{\epsilon}')\bar{\mathbf{B}}_\mathbf{e} + \bar{\mathbf{B}}_\mathbf{e}(\mathbb{H}^\mathbf{1} : D\boldsymbol{\epsilon}') + D\boldsymbol{\omega}\bar{\mathbf{B}}_\mathbf{e}\bar{\mathbf{B}}_\mathbf{e} - \bar{\mathbf{B}}_\mathbf{e}\bar{\mathbf{B}}_\mathbf{e}D\boldsymbol{\omega} \\ &= \mathbb{H}^\mathbf{2} : D\boldsymbol{\epsilon}' + D\boldsymbol{\omega}\bar{\mathbf{B}}_\mathbf{e}\bar{\mathbf{B}}_\mathbf{e} - \bar{\mathbf{B}}_\mathbf{e}\bar{\mathbf{B}}_\mathbf{e}D\boldsymbol{\omega} \end{aligned}$$

where

$$\mathbb{H}^2_{ijkl} = \frac{1}{2}(\delta_{ik}\bar{B}^e_{jm}\bar{B}^e_{ml} + \delta_{jl}\bar{B}^e_{im}\bar{B}^e_{mk} + \delta_{il}\bar{B}^e_{jm}\bar{B}^e_{mk} + \delta_{jk}\bar{B}^e_{im}\bar{B}^e_{ml}) + \bar{B}^e_{ik}\bar{B}^e_{jl} + \bar{B}^e_{il}\bar{B}^e_{jk}$$

The linearised invariants can be found as

$$\begin{aligned} D\bar{I}_1 &= D(\mathrm{tr}\bar{\mathbf{B}}_\mathbf{e}) = D(\mathbf{I} : \bar{\mathbf{B}}_\mathbf{e}) = \mathbf{I} : D\bar{\mathbf{B}}_\mathbf{e} \\ &= \mathbf{I} : (D\boldsymbol{\epsilon}'\bar{\mathbf{B}}_\mathbf{e} + \bar{\mathbf{B}}_\mathbf{e}D\boldsymbol{\epsilon}' + D\boldsymbol{\omega}\bar{\mathbf{B}}_\mathbf{e} - \bar{\mathbf{B}}_\mathbf{e}D\boldsymbol{\omega}) \\ &= 2tr(D\boldsymbol{\epsilon}'\bar{\mathbf{B}}_\mathbf{e}) + tr(D\boldsymbol{\omega}\bar{\mathbf{B}}_\mathbf{e}) - tr(\bar{\mathbf{B}}_\mathbf{e}D\boldsymbol{\omega}) \\ &= 2\mathbf{I} : D\boldsymbol{\epsilon}'\bar{\mathbf{B}}_\mathbf{e} \\ &= 2\bar{\mathbf{B}}_\mathbf{e} : D\boldsymbol{\epsilon}' \end{aligned}$$

$$\begin{aligned} D\bar{I}_2 &= \frac{1}{2}D(\bar{I}_1^2 - \mathrm{tr}(\bar{\mathbf{B}}_\mathbf{e}) = \frac{1}{2}(2\bar{I}_1 D\bar{I}_1 - \mathbf{I} : D(\bar{\mathbf{B}}_\mathbf{e}\bar{\mathbf{B}}_\mathbf{e})) \\ &= 2\bar{I}_1\bar{\mathbf{B}}_\mathbf{e} : D\boldsymbol{\epsilon}' - \frac{1}{2}tr(\mathbb{H}^\mathbf{2} : D\boldsymbol{\epsilon}') \\ &= 2(\bar{I}_1\bar{\mathbf{B}}_\mathbf{e} - \bar{\mathbf{B}}_\mathbf{e}\bar{\mathbf{B}}_\mathbf{e}) : D\boldsymbol{\epsilon}' \end{aligned}$$

$$\begin{aligned} D\left(\frac{\partial W}{\partial \bar{I}_1}\right) &= \frac{\partial}{\partial \bar{I}_1}\left(\frac{\partial W}{\partial \bar{I}_1}\right) D\bar{I}_1 + \frac{\partial}{\partial \bar{I}_2}\left(\frac{\partial W}{\partial \bar{I}_1}\right) D\bar{I}_2 + \frac{\partial}{\partial J_e}\left(\frac{\partial W}{\partial \bar{I}_1}\right) DJ_e \\ &= 2\frac{\partial^2 W}{\partial \bar{I}_1^2}\bar{\mathbf{B}}_\mathbf{e} : D\boldsymbol{\epsilon}' + 2\frac{\partial^2 W}{\partial \bar{I}_1 \partial \bar{I}_2}(\bar{I}_1\bar{\mathbf{B}}_\mathbf{e} - \bar{\mathbf{B}}_\mathbf{e}\bar{\mathbf{B}}_\mathbf{e}) : D\boldsymbol{\epsilon}' + \frac{\partial^2 W}{\partial \bar{I}_1 \partial J_e}J_e D\epsilon_v \end{aligned}$$

$$
\begin{aligned}
D\left(\frac{\partial W}{\partial \bar{I}_2}\right) &= \frac{\partial}{\partial \bar{I}_1}\left(\frac{\partial W}{\partial \bar{I}_2}\right) D\bar{I}_1 + \frac{\partial}{\partial \bar{I}_2}\left(\frac{\partial W}{\partial \bar{I}_2}\right) D\bar{I}_2 + \frac{\partial}{\partial J_e}\left(\frac{\partial W}{\partial \bar{I}_2}\right) DJ_e \\
&= 2\frac{\partial^2 W}{\partial \bar{I}_1 \partial \bar{I}_2}\bar{\mathbf{B}}_\mathbf{e} : D\boldsymbol{\epsilon}' + 2\frac{\partial^2 W}{\partial \bar{I}_2^2}(\bar{I}_1\bar{\mathbf{B}}_\mathbf{e} - \bar{\mathbf{B}}_\mathbf{e}\bar{\mathbf{B}}_\mathbf{e}) : D\boldsymbol{\epsilon}' + \frac{\partial^2 W}{\partial \bar{I}_2 \partial J_e} J_e D\epsilon_v
\end{aligned}
$$

We are now equipped to find the terms in the linearised virtual work equation

$$D(J\boldsymbol{\sigma}') = (DJ)\boldsymbol{\sigma}' + J(D\boldsymbol{\sigma}')$$

$$
\begin{aligned}
\boldsymbol{\sigma}' &= \boldsymbol{\sigma} - \frac{1}{3}\mathrm{tr}(\boldsymbol{\sigma})\mathbf{I} \\
&= \frac{2}{J}\left[\left(\frac{\partial W}{\partial \bar{I}_1} + \bar{I}_1\frac{\partial W}{\partial \bar{I}_2}\right)\bar{\mathbf{B}}_\mathbf{e} - \frac{\partial W}{\partial \bar{I}_2}\bar{\mathbf{B}}_\mathbf{e}\bar{\mathbf{B}}_\mathbf{e} - \frac{1}{3}\left(\bar{I}_1\frac{\partial W}{\partial \bar{I}_1} + 2\bar{I}_2\frac{\partial W}{\partial \bar{I}_2}\right)\mathbf{I}\right] - \frac{J_e}{J}\frac{\partial W}{\partial J_e}\mathbf{I} \\
&- \frac{1}{3}\left(\frac{2}{J}\left[\left(\frac{\partial W}{\partial \bar{I}_1} + \bar{I}_1\frac{\partial W}{\partial \bar{I}_2}\right)tr(\bar{\mathbf{B}}_\mathbf{e})\mathbf{I} - \frac{\partial W}{\partial \bar{I}_2}tr(\bar{\mathbf{B}}_\mathbf{e}\bar{\mathbf{B}}_\mathbf{e})\mathbf{I} - \frac{1}{3}\left(\bar{I}_1\frac{\partial W}{\partial \bar{I}_1} + 2\bar{I}_2\frac{\partial W}{\partial \bar{I}_2}\right)tr(\mathbf{I})\mathbf{I}\right] - \frac{J_e}{J}\frac{\partial W}{\partial J_e}tr(\mathbf{I})\mathbf{I}\right) \\
&= \frac{2}{J}\left[\left(\frac{\partial W}{\partial \bar{I}_1} + \bar{I}_1\frac{\partial W}{\partial \bar{I}_2}\right)(\bar{\mathbf{B}}_\mathbf{e} - \frac{1}{3}\bar{I}_1\mathbf{I}) - \frac{\partial W}{\partial \bar{I}_2}(\bar{\mathbf{B}}_\mathbf{e}\bar{\mathbf{B}}_\mathbf{e} - \frac{1}{3}tr(\bar{\mathbf{B}}_\mathbf{e}\bar{\mathbf{B}}_\mathbf{e})\mathbf{I})\right]
\end{aligned}
$$

$$
\begin{aligned}
D\boldsymbol{\sigma}' = {} & D(\frac{2}{J})\left[\left(\frac{\partial W}{\partial \bar{I}_1} + \bar{I}_1\frac{\partial W}{\partial \bar{I}_2}\right)(\bar{\mathbf{B}}_\mathbf{e} - \frac{1}{3}\bar{I}_1\mathbf{I}) - \frac{\partial W}{\partial \bar{I}_2}(\bar{\mathbf{B}}_\mathbf{e}\bar{\mathbf{B}}_\mathbf{e} - \frac{1}{3}tr(\bar{\mathbf{B}}_\mathbf{e}\bar{\mathbf{B}}_\mathbf{e})\mathbf{I})\right] \\
& + \frac{2}{J}\left[\left(D(\frac{\partial W}{\partial \bar{I}_1}) + D(\bar{I}_1)\frac{\partial W}{\partial \bar{I}_2} + \bar{I}_1 D(\frac{\partial W}{\partial \bar{I}_2})\right)(\bar{\mathbf{B}}_\mathbf{e} - \frac{1}{3}\bar{I}_1\mathbf{I}) + \left(\frac{\partial W}{\partial \bar{I}_1} + \bar{I}_1\frac{\partial W}{\partial \bar{I}_2}\right)(D\bar{\mathbf{B}}_\mathbf{e} - \frac{1}{3}(BarI_1)\mathbf{I})\right] \\
& - D(\frac{\partial W}{\partial \bar{I}_2})\left[(\bar{\mathbf{B}}_\mathbf{e}\bar{\mathbf{B}}_\mathbf{e} - \frac{1}{3}tr(\bar{\mathbf{B}}_\mathbf{e}\bar{\mathbf{B}}_\mathbf{e})\mathbf{I})\right] - \frac{\partial W}{\partial \bar{I}_2}\left[D(\bar{\mathbf{B}}_\mathbf{e}\bar{\mathbf{B}}_\mathbf{e}) - \frac{1}{3}D(tr(\bar{\mathbf{B}}_\mathbf{e}\bar{\mathbf{B}}_\mathbf{e}))\mathbf{I}\right]
\end{aligned}
$$

We use the following simplifications.

$$
\begin{aligned}
&(\bar{\mathbf{B}}_\mathbf{e} : D\boldsymbol{\epsilon}')\bar{\mathbf{B}}_\mathbf{e} = \bar{B}^e_{ij}\bar{B}^e_{kl}D\epsilon'_{kl} = (\bar{\mathbf{B}}_\mathbf{e} \otimes \bar{\mathbf{B}}_\mathbf{e}) : D\boldsymbol{\epsilon}' \\
&(\bar{\mathbf{B}}_\mathbf{e} \cdot \bar{\mathbf{B}}_\mathbf{e} : D\boldsymbol{\epsilon}')\bar{\mathbf{B}}_\mathbf{e} = \bar{B}^e_{ij}\bar{B}^e_{kp}\bar{B}^e_{pl}D\epsilon'_{kl} = (\bar{\mathbf{B}}_\mathbf{e} \otimes \bar{\mathbf{B}}_\mathbf{e} \cdot \bar{\mathbf{B}}_\mathbf{e}) : D\boldsymbol{\epsilon}' \\
&(\bar{\mathbf{B}}_\mathbf{e} : D\boldsymbol{\epsilon}')(\bar{\mathbf{B}}_\mathbf{e} \cdot \bar{\mathbf{B}}_\mathbf{e}) = \bar{B}^e_{ip}\bar{B}^e_{pj}\bar{B}^e_{kl}D\epsilon'_{kl} = (\bar{\mathbf{B}}_\mathbf{e} \cdot \bar{\mathbf{B}}_\mathbf{e} \otimes \bar{\mathbf{B}}_\mathbf{e}) : D\boldsymbol{\epsilon}' \\
&(\bar{\mathbf{B}}_\mathbf{e} \cdot \bar{\mathbf{B}}_\mathbf{e} : D\boldsymbol{\epsilon}')(\bar{\mathbf{B}}_\mathbf{e} \cdot \bar{\mathbf{B}}_\mathbf{e}) = \bar{B}^e_{ip}\bar{B}^e_{pj}\bar{B}^e_{kq}\bar{B}^e_{ql}D\epsilon'_{kl} = (\bar{\mathbf{B}}_\mathbf{e} \cdot \bar{\mathbf{B}}_\mathbf{e} \otimes \bar{\mathbf{B}}_\mathbf{e} \cdot \bar{\mathbf{B}}_\mathbf{e}) : D\boldsymbol{\epsilon}' \\
&(\mathbf{I} : D\boldsymbol{\epsilon}')\bar{\mathbf{B}}_\mathbf{e} = \bar{B}^e_{ij}\delta_{kl}D\epsilon'_{kl} = (\bar{\mathbf{B}}_\mathbf{e} \otimes \mathbf{I}) : D\boldsymbol{\epsilon}' \\
&(\bar{\mathbf{B}}_\mathbf{e} : D\boldsymbol{\epsilon}')\mathbf{I} = \delta_{ij}\bar{B}^e_{kl}D\epsilon'_{kl} = (\mathbf{I} \otimes \bar{\mathbf{B}}_\mathbf{e}) : D\boldsymbol{\epsilon}' \\
&(\mathbf{I} : D\boldsymbol{\epsilon}')(\bar{\mathbf{B}}_\mathbf{e} \cdot \bar{\mathbf{B}}_\mathbf{e}) = \bar{B}^e_{ip}\bar{B}^e_{pj}\delta_{kl}D\epsilon'_{kl} = (\bar{\mathbf{B}}_\mathbf{e} \cdot \bar{\mathbf{B}}_\mathbf{e} \otimes \mathbf{I}) : D\boldsymbol{\epsilon}' \\
&(\bar{\mathbf{B}}_\mathbf{e} \cdot \bar{\mathbf{B}}_\mathbf{e} : D\boldsymbol{\epsilon}')\mathbf{I} = \delta_{ij}\bar{B}^e_{kp}\bar{B}^e_{pl}D\epsilon'_{kl} = (\mathbf{I} \otimes \bar{\mathbf{B}}_\mathbf{e} \cdot \bar{\mathbf{B}}_\mathbf{e}) : D\boldsymbol{\epsilon}'
\end{aligned}
$$

On substituting these, and keeping symmetry in mind we get

$$D(J\boldsymbol{\sigma}') = J(\mathbb{C}^s : D\boldsymbol{\epsilon}' + \mathbf{Q}D\epsilon_v + D\boldsymbol{\omega} \cdot \boldsymbol{\sigma}' - \boldsymbol{\sigma}' \cdot D\boldsymbol{\omega})$$

where

$$
\begin{aligned}
\mathbb{C}^s = &\frac{2}{J}\left(\frac{\partial W}{\partial \bar{I}_1} + \bar{I}_1\frac{\partial W}{\partial \bar{I}_2}\right)\mathbb{H}^1 - \frac{\partial W}{\partial \bar{I}_2}\mathbb{H}^2 + \frac{4}{J}\left(\frac{\partial^2 W}{\partial \bar{I}_1^2} + 2\bar{I}_1\frac{\partial^2 W}{\partial \bar{I}_1\partial \bar{I}_2} + \bar{I}_1^2\frac{\partial^2 W}{\partial \bar{I}_2^2}\right)\bar{\mathbf{B}}_\mathbf{e} \otimes \bar{\mathbf{B}}_\mathbf{e} \\
&- \frac{4}{J}\frac{\partial^2 W}{\partial \bar{I}_1\partial \bar{I}_2}(\bar{\mathbf{B}}_\mathbf{e} \otimes \bar{\mathbf{B}}_\mathbf{e} \cdot \bar{\mathbf{B}}_\mathbf{e} + \bar{\mathbf{B}}_\mathbf{e} \cdot \bar{\mathbf{B}}_\mathbf{e} \otimes \bar{\mathbf{B}}_\mathbf{e}) + \frac{4}{J}\frac{\partial^2 W}{\partial \bar{I}_2^2}\bar{\mathbf{B}}_\mathbf{e} \cdot \bar{\mathbf{B}}_\mathbf{e} \otimes \bar{\mathbf{B}}_\mathbf{e} \cdot \bar{\mathbf{B}}_\mathbf{e} \\
&- \frac{4}{3J}\left[\frac{\partial W}{\partial \bar{I}_1} + 2\bar{I}_1\frac{\partial W}{\partial \bar{I}_2} + \bar{I}_1^2\frac{\partial^2 W}{\partial \bar{I}_1^2} + (\bar{I}_1^2 + 2\bar{I}_2)\frac{\partial^2 W}{\partial \bar{I}_1\partial \bar{I}_2} + 2\bar{I}_1\bar{I}_2\frac{\partial^2 W}{\partial \bar{I}_2^2}\right](\mathbf{I} \otimes \bar{\mathbf{B}}_\mathbf{e} + \bar{\mathbf{B}}_\mathbf{e} \otimes \mathbf{I}) \\
&+ \frac{4}{3J}\left(2\frac{\partial W}{\partial \bar{I}_1} + 2\bar{I}_1\frac{\partial^2 W}{\partial \bar{I}_1\partial \bar{I}_2} + 2\bar{I}_2\frac{\partial^2 W}{\partial \bar{I}_2^2}\right)(\mathbf{I} \otimes \bar{\mathbf{B}}_\mathbf{e} \cdot \bar{\mathbf{B}}_\mathbf{e} + \bar{\mathbf{B}}_\mathbf{e} \cdot \bar{\mathbf{B}}_\mathbf{e} \otimes \mathbf{I})
\end{aligned}
$$

$$\mathbf{Q} = 2\left(\frac{\partial^2 W}{\partial \bar{I}_1\partial J_e} + \bar{I}_1\frac{\partial^2 W}{\partial \bar{I}_2\partial J_e}\right)\bar{\mathbf{B}}_\mathbf{e} - 2\frac{\partial^2 W}{\partial \bar{I}_2\partial J_e}\bar{\mathbf{B}}_\mathbf{e} \cdot \bar{\mathbf{B}}_\mathbf{e} - \frac{2}{3}\left(\bar{I}_1\frac{\partial^2 W}{\partial \bar{I}_1\partial J_e} + 2\bar{I}_2\frac{\partial^2 W}{\partial \bar{I}_2\partial J_e}\right)\mathbf{I}$$

Also,

$$D(Jp) = -J(\mathbf{Q} : D\boldsymbol{\epsilon}' + KD\epsilon_v)$$

where

$$K = J_e \frac{\partial^2 W}{\partial J_e^2} + \frac{\partial W}{\partial J_e}$$

The last two terms in the linearised virtual work equation can be written as

$$\begin{aligned}
\boldsymbol{\sigma}' : D(\delta\boldsymbol{\epsilon}') - pD(\delta\epsilon_v) &= (\boldsymbol{\sigma} + p\mathbf{I}) : D(\delta\boldsymbol{\epsilon} - \frac{1}{3}\delta\epsilon_v\mathbf{I}) - pD(\delta\epsilon_v) \\
&= \boldsymbol{\sigma} : D(\delta\boldsymbol{\epsilon} - \boldsymbol{\sigma} : \frac{1}{3}\delta\epsilon_v\mathbf{I} - pD(\delta\epsilon_v) \\
&= \boldsymbol{\sigma} : D(\delta\boldsymbol{\epsilon})
\end{aligned}$$

This can be simplified further as

$$\begin{aligned}
\boldsymbol{\sigma} : D(\delta\boldsymbol{\epsilon}) = \sigma_{ij} D\delta\epsilon_{ij} &= \sigma_{ij}\frac{1}{2}(D\delta L_{ij} + D\delta L_{ji}) \\
&= \sigma_{ij} D\delta_{ij} \\
&= \sigma_{ij} D\frac{\partial \delta u_i}{\partial x_j} = \sigma_{ij} D\frac{\partial \delta u_i}{\partial X_j} DF^{-1}_{kj} \\
&= -\sigma_{ij} D\frac{\partial \delta u_i}{\partial X_j} F^{-1}_{kp} DF_{pm} F^{-1}_{mj} \\
&= -\sigma_{ij}\frac{\partial \delta u_i}{\partial x_p}\frac{\partial Du_p}{\partial x_j} \\
&= -\sigma_{ij}\delta L_{ip} DL_{pj}
\end{aligned}$$

The term with rotational part of $D(J\boldsymbol{\sigma}')$ can be simplified as

$$\begin{aligned}
(D\boldsymbol{\omega}\cdot\boldsymbol{\sigma}' - \boldsymbol{\sigma}'\boldsymbol{\omega}) : \delta\boldsymbol{\epsilon}' &= (D\boldsymbol{\omega}\cdot\boldsymbol{\sigma} + D\boldsymbol{\omega}\cdot p\mathbf{I} - \boldsymbol{\sigma}\boldsymbol{\omega} - p\mathbf{I}\boldsymbol{\omega}) : \delta\boldsymbol{\epsilon}' \\
&= (D\boldsymbol{\omega}\cdot\boldsymbol{\sigma} - \boldsymbol{\sigma}\boldsymbol{\omega}) : \delta\boldsymbol{\epsilon}' \\
&= D\omega_{ik}\sigma_{kj}\delta\epsilon_{ij} - \sigma_{ik}D\omega_{kj}\delta\epsilon_{ij} \\
&= -2\sigma_{ik}D\omega_{kj}\delta\epsilon_{ij} \\
&= -2\sigma_{ik}(-D\epsilon_{kj} + DL_{kj})\delta\epsilon_{ij} \\
&= 2\sigma_{ik}D\epsilon_{kj}\delta\epsilon_{ij} - \sigma_{ik}DL_{kj}\delta L_{ij} - \sigma_{ik}DL_{kj}\delta L_{ji}
\end{aligned}$$

The two terms above can now be combined together as

$$\boldsymbol{\sigma}' : D(\delta\boldsymbol{\epsilon}') - pD(\delta\epsilon_v) + (D\boldsymbol{\omega}\cdot\boldsymbol{\sigma}' - \boldsymbol{\sigma}'\boldsymbol{\omega}) : \delta\boldsymbol{\epsilon}' = -\boldsymbol{\sigma} : (2\delta\epsilon\cdot D\epsilon - \delta\mathbf{L}^T\cdot D\mathbf{L})$$

This terms arises due to geometric stiffness and is already accounted for by ABAQUS. The remainder of the linearised virtual work equation constitutes the material stiffness which we give as input to ABAQUS through UMAT. The material tangent stiffness is defined as:

$$\begin{aligned} DDSDDE &= \frac{1}{J}\frac{D(J\boldsymbol{\sigma})}{D\boldsymbol{\epsilon}} = \frac{1}{J}\left[\frac{D(J\boldsymbol{\sigma})}{D\boldsymbol{\epsilon}'} : \frac{D\boldsymbol{\epsilon}'}{D\boldsymbol{\epsilon}} + \frac{D(J\boldsymbol{\sigma})}{D\epsilon_v}\otimes\frac{D\epsilon_v}{D\boldsymbol{\epsilon}}\right] \\ &= \frac{1}{J}\left[\frac{D(J\boldsymbol{\sigma}')}{D\boldsymbol{\epsilon}'} : \frac{D\boldsymbol{\epsilon}'}{D\boldsymbol{\epsilon}} - \frac{D(Jp\mathbf{I})}{D\boldsymbol{\epsilon}'} : \frac{D\boldsymbol{\epsilon}'}{D\boldsymbol{\epsilon}} + \frac{D(J\boldsymbol{\sigma}')}{D\epsilon_v}\otimes\frac{D\epsilon_v}{D\boldsymbol{\epsilon}} - \frac{D(Jp\mathbf{I})}{D\epsilon_v}\otimes\frac{D\epsilon_v}{D\boldsymbol{\epsilon}}\right] \end{aligned}$$

$$DDSDDE_{ijkl} = \frac{1}{J}\left[\frac{D(J\sigma'_{ij})}{D\epsilon'_{pq}} : \frac{D\epsilon'_{pq}}{D\epsilon_{kl}} - \frac{D(Jp\delta_{ij})}{D\epsilon'_{pq}} : \frac{D\epsilon'_{pq}}{D\epsilon_{kl}} + \frac{D(J\sigma'_{ij})}{D\epsilon_v}\otimes\frac{D\epsilon_v}{D\epsilon_{kl}} - \frac{D(Jp\delta_{ij})}{D\epsilon_v}\otimes\frac{D\epsilon_v}{D\epsilon_{kl}}\right]$$

$$\begin{aligned} \frac{D\epsilon'_{pq}}{D\epsilon_{kl}} &= \frac{D}{D\epsilon_{kl}}(\epsilon_{pq} - \frac{1}{3}\delta_{ij}\epsilon_{ij}\delta_{pq}) = \delta_{pk}\delta_{ql} - \frac{1}{3}\delta_{pq}\delta_{kl} \\ \frac{D\epsilon_v}{D\epsilon_{kl}} &= \frac{D\delta_{ij}\epsilon_{ij}}{D\epsilon_{kl}} = \frac{D\epsilon_{ii}}{D\epsilon_{kl}} = \delta_{kl} \end{aligned}$$

$$\begin{aligned} DDSDDE_{ijkl} &= \mathbb{C}^s_{ijpq}\delta_{pk}\delta_{ql} - \frac{1}{3}\mathbb{C}^s_{ijpq}\delta_{pq}\delta kl + \delta_{ij}Q_{kl} + Q_{ij}\delta_{kl} + K\delta_{ij}\delta_{kl} \\ &= \mathbb{C}^s_{ijkl} - \frac{1}{3}\mathbb{C}^s_{ijpp}\delta kl + \delta_{ij}Q_{kl} + Q_{ij}\delta_{kl} + K\delta_{ij}\delta_{kl} \end{aligned}$$

For updating the stresses, our UMAT uses the expression for stresses that we have obtained before, rather than an iterative stress update term. In order to incorporate incompressibility, we use a very small value of $D_1 = 10^{-8}Pa^{-1}$.

Bibliography

[1] ABAQUS (2011). *Abaqus 6.11 Online Documentation*. Dassault Systemes.

[2] Ambrosi, D., Ateshian, G., Arruda, E., Cowin, S., Dumais, J., Goriely, A., Holzapfel, G., Humphrey, J., Kemkemer, R., Kuhl, E., Olberding, J., Taber, L., and Garikipati, K. (2011). Perspectives on biological growth and remodeling. *Journal of the Mechanics and Physics of Solids*, 59(4):863–883.

[3] Dervaux, J. and Ben Amar, M. (2008). Morphogenesis of growing soft tissues. *Phys. Rev. Lett.*, 101(6):068101.

[4] Durel, J. F. and Nerurkar, N. L. (2020). Mechanobiology of vertebrate gut morphogenesis. *Curr. Opin. Genet. Dev.*, 63:45–52.

[5] G. Himpel, E. Kuhl, A. M. P. S. (2005). Computational modelling of isotropic multiplicative growth. *Computer Modeling in Engineering & Sciences*, 8(2):119–134.

[6] Halder, S. (2017). Mechanics of a growing hyperelastic mass: A study of the morphogenesis of vertebrate forebrain.

[7] Liang, H. and Mahadevan, L. (2009). The shape of a long leaf. *Proc. Natl. Acad. Sci. U. S. A.*, 106(52):22049–22054.

[8] Lubarda, V. and Hoger, A. (2002). On the mechanics of solids with a growing mass. *International Journal of Solids and Structures*, 39(18):4627–4664.

[9] Nerurkar, N. L., Mahadevan, L., and Tabin, C. J. (2017). BMP signaling controls buckling forces to modulate looping morphogenesis of the gut. *Proc. Natl. Acad. Sci. U. S. A.*, 114(9):2277–2282.

[10] Nguyen, N. and Waas, A. M. (2016). Nonlinear, finite deformation, finite element analysis. *Zeitschrift für angewandte Mathematik und Physik*, 67(3):35.

[11] Rodriguez, E. K., Hoger, A., and McCulloch, A. D. (1994). Stress-dependent finite growth in soft elastic tissues. *Journal of Biomechanics*, 27(4):455–467.

[12] Shyer, A. E., Tallinen, T., Nerurkar, N. L., Wei, Z., Gil, E. S., Kaplan, D. L., Tabin, C. J., and Mahadevan, L. (2013). Villification: how the gut gets its villi. *Science*, 342(6155):212–218.

[13] Tozluoğlu, M. and Mao, Y. (2020). On folding morphogenesis, a mechanical problem. *Philos Trans R Soc Lond B Biol Sci*, 375(1809):20190564.

[14] Wyczalkowski, M. A., Chen, Z., Filas, B. A., Varner, V. D., and Taber, L. A. (2012). Computational models for mechanics of morphogenesis. *Birth Defects Res. C Embryo Today*, 96(2):132–152.